POLITECNICO DI TORINO
Repository ISTITUZIONALE

Uncertainties in Small-Strain Damping Ratio Evaluation and Their Influence on Seismic Ground Response Analyses

Original
Uncertainties in Small-Strain Damping Ratio Evaluation and Their Influence on Seismic Ground Response Analyses / Foti, S., Aimar, M., Ciancimino, A. (SPRINGER TRANSACTIONS IN CIVIL AND ENVIRONMENTAL ENGINEERING). - In: Latest Developments in Geotechnical Earthquake Engineering and Soil DynamicsELETTRONICO. - [s.l] : Springer, 2021. - ISBN 978-981-16-1467-5. - pp. 175-213 [10.1007/978-981-16-1468-2_9]

Availability:
This version is available at: 11583/2926832 since: 2021-09-28T10:12:28Z

Publisher:
Springer

Published
DOI:10.1007/978-981-16-1468-2_9

Terms of use:

This article is made available under terms and conditions as specified in the corresponding bibliographic description in the repository

Publisher copyright

(Article begins on next page)

27 November 2026

Uncertainties in Small-Strain Damping Ratio Evaluation and Their Influence on Seismic Ground Response Analyses

Sebastiano Foti[1][0000-0003-4505-5091], Mauro Aimar[1][0000-0002-1170-9774] and Andrea Ciancimino[1][0000-0001-8955-4605]

[1] Politecnico di Torino, Turin, Italy

Abstract. The ground response to seismic waves is governed by the geometry and the mechanical properties of the site. A proper characterization of the soil behavior is thus a fundamental aspect and it should account for the uncertainties associated with the model parameters. In particular, the quantification of the small-strain damping is a critical task, especially in low to moderate seismicity areas. In the present paper, the main issues related to the definition of the damping at small strains are firstly treated in the light of the biases affecting both laboratory and in situ tests. Higher values of damping are in fact expected in field, where wave scattering phenomena take place. The influence of the parameter on the overall site response is subsequently assessed by means of a stochastic database of Ground Response Analyses. The results highlight a reduction of the expected ground motion at the surface, especially for deep and soft sites, when a site-based small-strain damping is selected. Finally, the differences between site and laboratory values are analyzed with reference to a specific case study. The influence of the damping at small strains resulted to be comparable or even higher with respect to the uncertainties related to the shear wave velocity profile and the modulus reduction and damping curves. Therefore, a proper evaluation of the uncertainties in the small-strain damping evaluation should not be neglected.

Keywords: Small-strain damping, Ground Response Analysis, Uncertainties.

1 Introduction

A proper evaluation of site effects is crucial to define the expected ground motion at the surface. Local site conditions modify the shaking characteristics due to variations of mechanical properties and basin/surface geometry. Site effects are therefore referred, respectively, as stratigraphic and geometrical amplification (e.g., [1-3]).

Site response studies are usually performed to quantify the differences between the surface ground motion and the reference condition (i.e., flat rock-outcropping formation) where no amplification phenomena are expected. Different methods can be used to evaluate site effects: studies based on recorded ground motions (i.e., data-based approach) or numerical simulations (i.e., simulation-based approach). In the absence of

a sufficient number of available records at the site, the latter represents the only feasible option [4-6].

The complex phenomena affecting the seismic waves propagation can be represented through one-, two- and three-dimensional site response analyses, accordingly to the specific features of the site. 1-D Ground Response Analyses (hereafter, GRAs) are based on the assumption of vertical propagation of shear waves through a horizontally stratified medium. The applicability of this assumption is constrained by the geometry of the site: when no major basin or topographic effects are expected, GRAs are considered to be adequate to model the site response [3; 7]. Several studies have addressed the actual capabilities of 1-D approaches in predicting the mean site response and, notwithstanding the well-known limitations, GRAs are still the primary choice for the assessment of site effects (e.g., [7-15]).

Leaving aside the dimensionality of the problem, an adequate simulation of the propagation of seismic waves cannot disregard the actual stress-strain response of soils under cyclic loading. The reference parameters (termed as dynamic properties) adopted to describe the behavior of soils are usually the secant shear modulus (G_S) and the material damping ratio (D). The latter represents the energy internally dissipated by the soil as a consequence of friction between soil particles, nonlinear soil behavior, and viscous effects. At very small strains, the soil response is practically linear, and G_S assumes its maximum value G_0. The energy dissipation, given in this range mainly by friction and viscosity, is almost constant and equal to the small-strain material damping ratio (D_0). For larger shear strains, nonlinearity in the stress-strain soil behavior leads to a G_S decay and, consequently, to an increase of the energy dissipation. The relationships between G_S/G_0 and D along with the cyclic shear strain amplitude (γ_c), are usually termed as modulus reduction and damping (MRD) curves [16].

The evaluation of the dynamic soil properties is carried out through geotechnical laboratory tests together with geophysical *in situ* tests. The reliability of laboratory measurements is in fact constrained by sample disturbance effects, which alter the structure of the soil affecting the shear-wave velocity V_S (and, then, the G_S) of the sample [17; 18]. The current state of practice is thus to evaluate the MRD curves in laboratory and adopt the V_S profile from specific *in situ* tests.

Different uncertainties and variabilities affect the results of GRAs due to both the approach adopted to model the complex nonlinear and inelastic response of soil and the selected model parameters [19]. As a consequence, the numerical simulations should be carried out within a probabilistic framework in order to Identify, Quantify, and Manage (i.e., IQM method [20]) all the uncertainties and variabilities involved in the analyses.

In the following, the main sources of uncertainties in GRAs are firstly analyzed in order to define the framework in which the uncertainties on D_0 are placed. The critical issues associated with the measurement of the small-strain damping are then identified in order to explain the differences observed between laboratory and *in situ* values. A review of approaches to evaluate the D_0 from field data is then reported. Finally, two different applications are presented to highlight the influence of D_0 on the outcomes of GRAs. Firstly, a stochastic database of GRAs is used to analyze the average response over a wide range of soil profiles. Subsequently, a specific well-documented case study

is considered to compare the impact of the D_0 variability to the effects of the uncertainties on V_S profile and MRD curves.

2 Sources of uncertainties in GRAs

Six factors can be identified as main sources of uncertainties in GRAs (after [21; 22]):

- shear-wave velocity profile;
- nonlinear approach;
- modulus reduction and damping curves;
- input motions;
- shear strength;
- small-strain damping ratio.

The V_S profile is the main parameter governing the wave propagation in the medium. It controls resonant frequencies and modifications of the motion at the interface. The V_S profile has to be based on adequate *in situ* geophysical measurements and the specific uncertainties associated to the test typology have to be carefully evaluated (further details can be found in [19] and [20]).

Different approaches can be used to model soil nonlinearity. A rigorous analysis should be based on a fully NonLinear (NL) approach, which allows for evaluating the actual stress-strain behavior in the time-domain. However, frequency-domain Equivalent Linear (EQL) analyses are commonly used to approximate the nonlinearity through an iterative approach based on the use of strain-compatible linear visco-elastic soil properties [23]. Finally, simplified Linear visco-Elastic (LE) analyses can be used to validate the model. The choice of an appropriate nonlinear approach depends on the expected shear strain level and/or on the possible development of excess pore-water pressure due to the coupling of shear and volumetric strains. The EQL procedure has the advantage to be stable and straightforward, but its applicability is constrained when soil layers undergo excessive shear strains (e.g., [13; 24]). Moreover, the time-independent assumption of the strain-compatible properties according to a predefined shear strain ratio is a further source of uncertainties [25]. On the other hand, NL analyses are more rigorous and of general applicability. Their practical use is anyway limited by the complexity of the approach and the consequent need of expert users (e.g., [7; 10; 15; 26]). The choice of an appropriate constitutive model and the parameter calibration is, indeed, crucial to obtain reliable results [27].

The MRD curves should be defined by means of specific laboratory tests. In absence of site-specific results, empirical models (e.g., [28-38]) can be used to predict the soil behavior as a function of different variables (e.g., soil type, Plasticity Index, mean confining pressure, Overconsolidation Ratio, loading frequency). The uncertainties on the empirical models related to the experimental variability of MRD curves and possible experimental errors can be quantified through the standard deviation provided along with the mean values (e.g., [33; 35; 38; 39]). Conversely, when laboratory tests are carried out, the main uncertainties are related to the experimental limitations and the

natural randomness of the soil properties at the site scale, associated to the geological spatial variation [40].

When very large strains occur, the MRD typically obtained with laboratory tests have to be corrected to cover the failure conditions (e.g., [41-43]). The main uncertainties in this regard are related to the randomness of the soil properties and to the specific tests performed to obtain the strength of the soil. Another source of uncertainties is related to the procedure adopted to merge the small- and large-strain behavior [11].

Real recorded ground motions are usually selected as input motions. The reference hazard condition is usually obtained with the Probabilistic Seismic Hazard Analysis (PSHA) [44], taking into account the source and path spatial variabilities through the spectral standard deviation. On the other side, the uncertainties related to the selection procedure are the choice of the hazard level, the type of reference spectrum, the spectral matching criterion and the type and number of inputs, along with the consistency with the reference condition [14; 22; 45].

Finally, uncertainties on the soil small-strain damping ratio D_0 have to be considered. The D_0 obtained by laboratory tests is associated with material energy dissipation. Therefore, the main uncertainties related to D_0 are the same as previously specified for the MRD curves. However, the applicability of D_0 values obtained through laboratory tests for GRAs has been questioned by different Authors (e.g., [14; 42; 46; 47]). Experimental evidence from back-analysis of Down-Hole seismic arrays showed, in fact, small-strain damping ratios in the field larger than the values obtained through laboratory tests (note that the small-strain damping ratio in field is hereafter referred as $D_{0,\,site}$, while D_0 is adopted for the material small-strain damping ratio measured in the laboratory). These differences have to be interpreted taking into account the energy dissipation mechanisms acting at the site scale. Wave scattering effects can modify the propagating seismic waves due to the heterogeneities in the soil profile [48; 49]. This phenomenon, which is relevant especially in the presence of large impedance contrasts [42], causes additional energy dissipation to the material dissipation and cannot be captured by laboratory tests. As a consequence, the $D_{0,\,site}$ should be adopted as small-strain damping when GRAs are performed. When no measurements of $D_{0,\,site}$ are available a procedure has to be adopted to correct the D_0 according to the expected values on site.

Although the uncertainties related to D_0 are usually referred as secondary [21; 22; 50], the choice of adequate values can strongly influence the soil response, especially in the small-strain field (e.g., [46; 51]). For instance, Boaga et al. [52] observed that D_0 affects the 1-D amplification in presence of strong impedance contrasts and its effect is more relevant at high frequencies, whereas its impact is smaller in soil deposits with smooth variations of the mechanical properties. Indeed, for increasing impedance ratio, the 1-D ground model exhibits a response closer to the theoretical case of homogeneous medium over a rigid bedrock, where the entity of the ground motion amplification is inversely proportional to D_0. Afshari and Stewart [53] tested the effect of three approaches to estimate $D_{0,\,site}$, based on seismological relations and the site decay parameter (κ_0), respectively. The assessment compared the observed response for low-intensity ground motions and the predicted one. They stated that the κ_0-informed $D_{0,\,site}$ provides a better fit between predicted and observed amplification than alternative damping models. On the other side, there is no consensus about the best approach for its

estimate and the proposed methods rely on data and resources that are often not available in common engineering applications. This difficulty has been highlighted by Stewart et al. [14], who suggested to deal the discrepancy between the $D_{0,\,site}$ and the laboratory-based D_0 as an epistemic uncertainty and to run a sensitivity study by assuming different variations ΔD, ranging between zero and 5%.

3 Laboratory Tests

Laboratory tests are often carried out to obtain the dynamic properties of soils. The different tests can be grouped into two main categories: cyclic tests, performed at low frequencies, and dynamic tests, carried out at higher frequencies. The most common cyclic tests are the Cyclic Triaxial (CTx) test, the Cyclic Torsional Shear (CTS) test and the Cyclic Direct Simple Shear (CDSS) test, along with its Double-Specimens (CDSDSS) variant. The stress-strain loops are directly used in cyclic tests to obtain the dynamic properties of the soil. On the other hand, a dynamic Resonant Column (RC) test can be performed to obtain the MRD curves analyzing the resonant conditions of the soil sample.

Results from laboratory tests were widely used in the past to identify the main parameters of the soil affecting, generally speaking, D and specifically D_0. For fine-grained soils, the D_0 is mainly influenced by the Plasticity Index (PI), the effective mean confining stress (σ'_m), and the OverConsolidation Ratio (OCR) [33]. Conversely, the relevant parameters for granular materials are the Uniformity Coefficient (C_u) and σ'_m [34]. Additionally, an open issue is represented by the influence of the loading frequency (f) (e.g., [33; 38; 54-58]).

In the following, the main features of the tests are firstly described, along with critical issues associated with the experimental measurement of D_0. A final remark is given about the dependency of D_0 from the loading frequency.

3.1 RC test

The RC test (ASTM D4015–15e1) is based on the theory of torsional waves propagation in the medium. The tests are usually carried out by means of modified versions of the free-fixed type apparatus described by Isenhower [60] and designed at the University of Texas at Austin.

Firstly, a cylindrical soil specimen is saturated, if required, through a back-pressure procedure. The consolidation phase takes then place, usually in isotropic conditions. Next, an electromagnetic driving system is used to excite the sample at the free top. The test is performed under loading control, applying torque loadings with increasing amplitudes. The bottom of the specimen is fixed in order to ensure adequate (i.e., well-defined) boundary conditions. For a given loading amplitude, several cycles are applied for variable frequencies over a wide range, in order to clearly identify the resonance condition of the first torsional mode of the specimen (f_0) associated to the cyclic shear strain reached. The soil response is tracked through an accelerometer installed in the top cap. The conditions are generally undrained and the pore-water pressure build-up

can be monitored. The test is able to investigate cyclic shear strain amplitudes ranging from 10^{-5} to 0.5 %.

The response of the soil to the dynamic excitation can be represented in terms of rotation (θ) vs frequency curve, where the frequency associated with the maximum amplitude θ_{max} is the f_0 of the sample. The V_S of the soil is then obtained via the equation of motion for torsional vibrations [61]:

$$\frac{I_\theta}{I_t} = \frac{2\pi f_0 h}{V_S} \cdot tan\left(\frac{2\pi f_0 h}{V_S}\right) \tag{1}$$

where I_θ is the mass polar moment of inertia of the specimen, I_t is the driving system polar moment of inertia and h is the height of the specimen.

The G_S can then be obtained through the well-known relationship:

$$G_S = \rho V_S{}^2 \tag{2}$$

being ρ the mass density of the soil.

Two different methods can be applied to define the damping ratio, namely the half-power bandwidth and the free-vibration decay method. In the half-power bandwidth method the connection between the shape of the frequency response curve and the dissipated energy is exploited (Fig. 1.a). It can be shown that, for small values of the damping ratio, the latter can be evaluated as:

$$D = \frac{f_2 - f_1}{f_0} \tag{3}$$

where f_1 and f_2 are the frequencies associated with a θ amplitude equal to $\sqrt{2}/2\,\theta_{max}$. The soil is assumed to behave linearly: the method is therefore reliable only in the small-strain range.

Alternatively, the free-vibration decay method can be used to obtain the damping ratio from the amplitude decay of the torsional oscillations. At the end of the test, after the application of the forced vibrations, the input current is switched off and the damped free vibrations of the sample are recorded by the accelerometer. By knowing two successive peak amplitudes (z_n and z_{n+1} corresponding, respectively, to the n-th and $n+1$-th cycle), the logarithmic decrement δ_{n+1} can be computed as:

$$\delta_{n+1} = ln\left(\frac{z_n}{z_{n+1}}\right) \tag{4}$$

The logarithmic decrement is computed for different successive cycles, then an average value (δ) is used to obtain the damping ratio as:

$$D = \frac{\delta}{2\pi} \tag{5}$$

The two methods are characterized by different advantages and disadvantages. When the free-vibrations method is used in the small-strain range, the background noise recorded by the accelerometer is not negligible and a filtering procedure has to be applied to the output signals prior to amplitude interpolation (Fig. 1.b). Moreover, given the small values of D_0, the difference between two consecutive peaks can be really small. As a consequence, the experimental standard deviation can be relatively high with respect to the average measured values.

On the other side, a well-recognized source of error in RC measurements of D from forced vibrations arises from the use of an electromagnetic driving system to provide the torsional excitation (e.g., [62-66]). The driving system is based on the interaction between the magnets and the magnetic field generated by the AC current passing through the solenoids. The driving torque applied to the sample is given by the resulting motion of the magnets. Meanwhile, the motion of the magnets induces an electromagnetic force which is opposed to the motion.

The phenomenon results in equipment-generated damping which is added to the actual material damping. The bias can be substantial, especially in the small-strain range where small values of material damping are expected. Different studies suggested correcting the results of the RC test by subtracting the equipment generated damping. The latter has to be obtained through a calibration procedure of the apparatus as a function of the loading frequency (e.g., [62; 63; 65]). However, the extent of the bias is not yet totally understood.

3.2 CTS and C(DS)DSS tests.

Despite the different configurations, the cyclic tests are all based on the same concept, i.e. to measure the dynamic properties directly from the stress-strain response of the soil (Fig. 2.a).

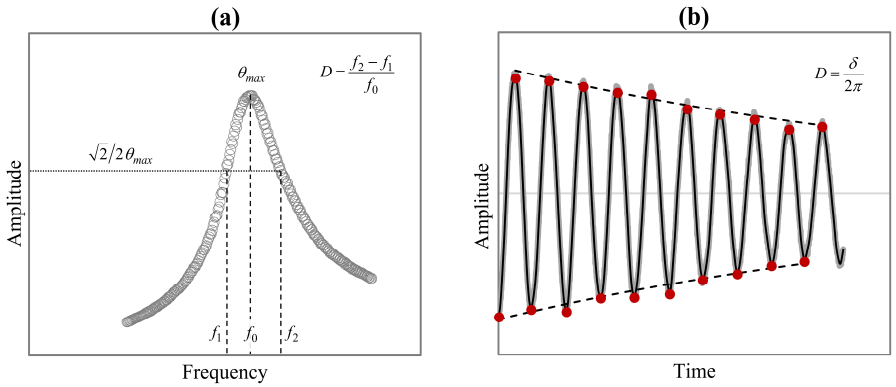

Fig. 1. Typical results of a RC test: (a) output amplitude vs frequency curve; (b) free-vibration decay plot.

The G_S is obtained as the average slope of the loop, while D can be computed in analogy with the critical damping ratio of a Single-Degree-Of-Freedom system constituted by a mass connected to a linearly elastic spring and a viscous dashpot. The stress-strain path for soils subjected to cyclic shear strains is indeed similar to the ellipse described by the SDOF system. Specifically, for a given loading-unloading cycle, D is evaluated as:

$$D = \frac{W_D}{4\pi W_S} \tag{6}$$

where W_D is the energy dissipated within one cycle and W_S is the maximum elastic strain energy.

In CTx tests (ASTM D3999/D3999M-11e1 and ASTM D5311/D5311M–13) a cylindrical specimen is firstly consolidated (either isotropically or anisotropically) in a standard triaxial cell. A cyclic deviator stress is then applied by keeping constant the cell pressure and changing the axial stress cyclically with a low loading frequency (about 1Hz).

The test is commonly performed under load-controlled conditions, but some devices are also equipped to perform displacement-controlled tests. The stresses and the strains are used to compute G_S and D. The applicability of the CTx test is generally restricted to relatively high shear strains (greater than 10^{-2} %) because of bedding errors and system compliance effects [3]. Local strain measurements can produce an increase of the accuracy of the device (e.g., [69-71]).

CTS tests can be performed in the same device used for RC tests. The driving system applies a fixed number of cycles for a given amplitude with a fixed loading frequency (usually between 0.1-0.5Hz). The rotation of the specimen is measured through a couple of displacement transducers connected to the top cap. The shear strain is then obtained from the rotation and, by knowing the input applied, it is possible to draw the loading-unloading loops.

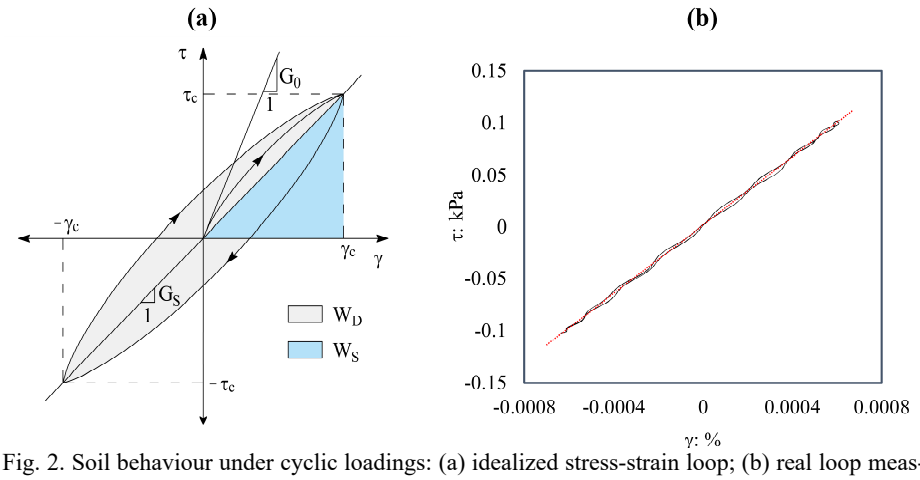

Fig. 2. Soil behaviour under cyclic loadings: (a) idealized stress-strain loop; (b) real loop measured in a CTS test at small strains.

Finally, in a CDSS test, a cylindrical specimen is cyclically loaded under displacement control by a horizontal piston. The test is performed in undrained conditions and the specimen cannot, usually, be consolidated at horizontal to vertical stress ratios different than K_0. The applicability of the test in the small-strain range is limited mainly because of frictional problems. The range can anyway be increased adopting a double specimen configuration [72]. The CDSDSS device is a modified version of the standard device designed by the Norwegian Geotechnical Institute [73] and it is able to capture the soil behavior also at very small strains [74].

The main issue regarding the cyclic tests is related to the measurement of the loops in the small-strain range. The stresses and the strains are indeed really small, and it becomes quite difficult to obtain a proper measurement even for the most apparatuses. For example, a loop measured during a CTS test, for a γ_c below the linearity threshold (i.e., in the almost linear branch of the stress-strain response) is showed in Fig. 2.b. It is clear that although is quite straightforward to define the G_0 from the slope of the loop, the small area inside the loop can be affected by the accuracy of the measurement. Consequently, the experimental relative error on D_0 can be, again, substantial.

3.3 Frequency-dependent soil behavior

The influence of the loading frequency on the material damping ratio is still an open issue. A number of experimental studies reported controversial results about the real extent of this dependency. Some studies also highlighted the possible impact of such dependency on GRAs (e.g., [75]).

Kim et al. [62] presented the results of RC and CTS tests on undisturbed samples of cohesive soil with a *PI* of 20-30%, showing that the small-strain damping ratio is almost linear for frequencies lower than 1Hz but increases at higher frequencies. Subsequently, Shibuya et al. [54] suggested the existence of three different branches. At low frequencies (<0.1Hz) the damping ratio tends to decrease with increasing frequencies. In the medium range (between 0.1 and 10 Hz, the typical seismic bandwidth) the damping is almost constant, irrespectively of the loading frequency. Finally, for higher frequencies D increases with f because of viscous effects. A similar trend was reported also by other studies, highlighting anyway a rate-dependency even in the seismic bandwidth (e.g., [18; 33; 34; 55; 57; 58]).

Such a trend is not so clearly identifiable at high strain amplitudes, where nonlinearity partially covers these aspects. Darendeli [33] proposed then to model the damping ratio curves of fine-grained soils by adding a strain-constant D_0 to the hysteretic damping ratio. The D_0 in the model depends on f. The latter has thus the effect of translating the damping curves. For granular dry materials, Kim and Stokoe [76] suggested that f has a negligible impact. Conversely, the effects become relevant for saturated specimens [34].

The motivation behind this behavior has to be found into the different mechanisms of energy dissipation taking place in soils during cyclic loadings (e.g., [54; 55]). In the very low-frequency range, the application of the load is quasi-static and creep phenomena occur. As a consequence, the slower is the application of the load, the higher is the D_0. Conversely, in the medium range, the dissipation is given mainly by the hysteretic

soil behavior that is almost frequency-independent. In the small-strain range anyway, a substantial component of the energy dissipation is attributed to pore fluid viscosity. The relative movement between the water and the soil skeleton generates viscous damping that is, obviously, frequency-dependent. At high frequencies thus the D_0 dramatically increases with f. This effect exists independently from the strain level, but it becomes less relevant at high strains when the hysteretic damping increases.

Ciancimino et al. [38] calibrated an empirical equation for predicting the D_0 of fine-grained soils from Central Italy. The equation, based on the model proposed by Darendeli [33], incorporates the dependency of D_0 from f in the range between 0.2 and 100 Hz:

$$D_0 = \left(\varphi_1 + \varphi_2 \cdot PI\right) \cdot {\sigma'_m}^{\varphi_3} \cdot \left[1 + \varphi_4 \cdot ln\left(f\right)\right] \tag{7}$$

where φ_{1-4} are model parameters equal, respectively, to 1.281, 0.036, -0.274, and 0.134, PI is expressed in percentage, f in Hz, and σ'_m in atm. The equation is conceived to model the viscous component but neglects the creep effects at low frequencies.

The Authors also suggested a possible application of this equation to correct the results of a laboratory test by taking into account the loading frequency. The procedure is relevant especially for RC tests, usually carried out at frequencies not representative of the typical seismic bandwidth.

However, it is worth noting that subtracting a constant value of D_0 from the damping curve obtained in a RC test is not completely correct. The RC test is in fact carried out at variable frequencies, according to the resonance conditions for different strain amplitudes. The steps below have to be followed to correct the experimental damping curve to a frequency of 1Hz:

- the experimental $D_0\left(f_1\right)$ measured at the first shear strain amplitude is normalized to a frequency of 1Hz, by dividing it by $\left[1 + \varphi_4 \cdot ln\left(f_1\right)\right]$, where f_1 is the first loading frequency;
- from each i-th point of the damping curve is subtracted the corresponding $D_0\left(f_i\right)$, computed as $D_0\left(1Hz\right) \cdot \left[1 + \varphi_4 \cdot ln\left(f_i\right)\right]$, where f_i is the i-th loading frequency;
- finally, $D_0\left(1Hz\right)$ is added to the $D - D_0$ curve previously computed in order to obtain the frequency-normalized damping curve $D\left(1Hz\right)$.

In Fig. 3 an example of the normalization procedure for a RC test is reported. Fig. 3.a shows the initial comparison between a RC and a CTS test carried out on the same sample (Massa Fermana BH1S1 sample, from [38]). A marked difference is observed, especially in the small-strain range. The results of the two tests are then corrected to match a frequency of 1Hz (Fig. 3.b reports the procedure for the RC test). The correction is clearly less significant for the CTS test performed at a constant frequency of 0.1 Hz. Finally, in Fig. 3.c the normalized results are compared, showing good agreement.

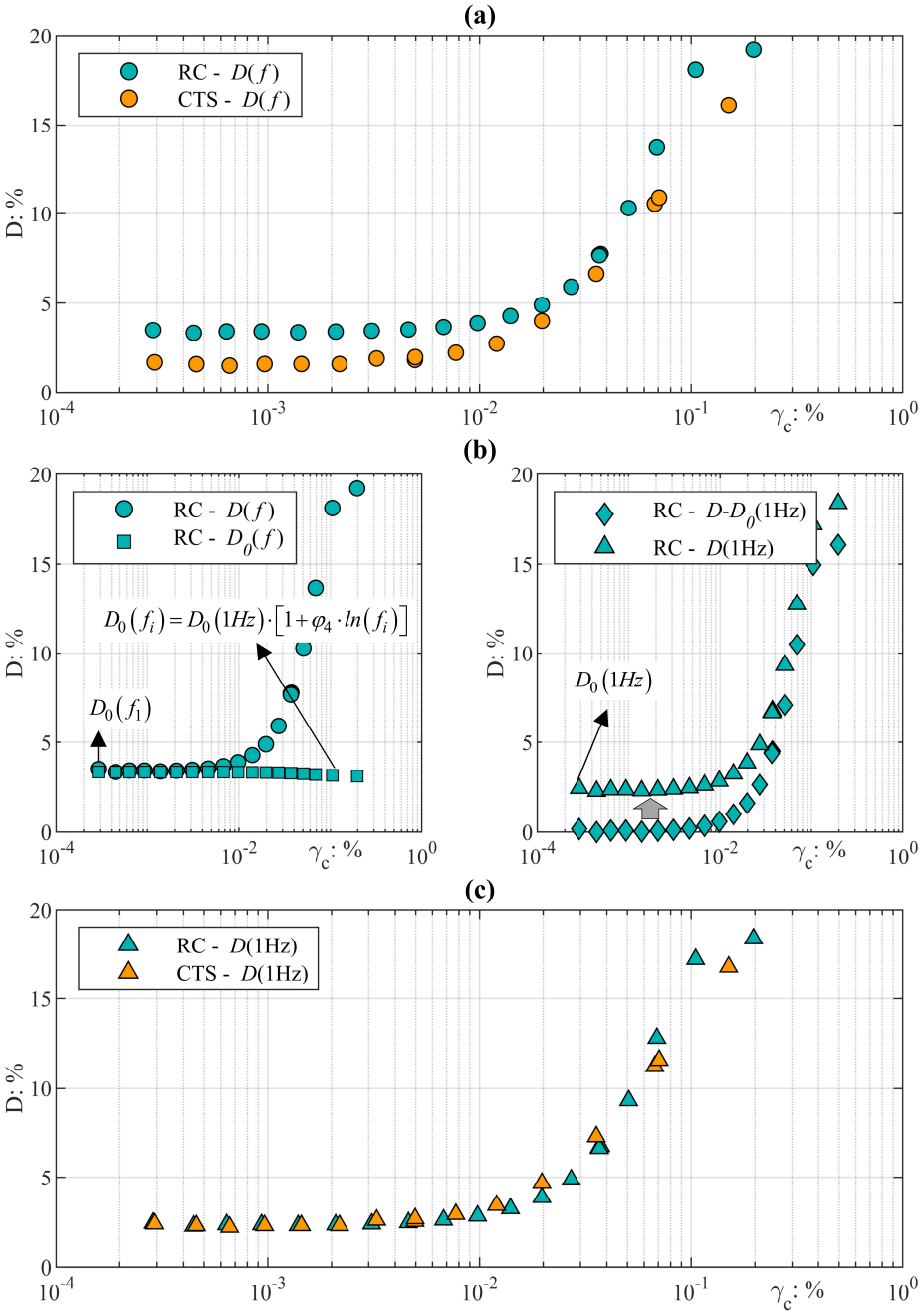

Fig. 3 Effectiveness of the normalization procedure: (a) comparison between RC and TC results; (b) normalization procedure for the RC test; (c) comparison of the normalized curves (modified from [38]).

The proposed approach can be applied also to other predictive models, provided that D_0 is given as a function of f (e.g., [33]). Anyway, it has to be pointed out that although the procedure is presented as a correction for the loading frequency, it is to some extent a correction for the type of test. As a matter of fact, tests performed at low loading frequencies are always cyclic tests, while at higher frequencies just RC tests can be carried out. As a consequence, the dependency of D_0 from f cannot be easily separated from other possible sources of discrepancies between cyclic and RC tests.

A possible alternative is given by the so-called Non-Resonance Column (N-RC) method ([58; 77-79]). The method is based on the experimental measurement of the complex shear modulus $G_S^*(f)$ of a soil specimen, idealized as a linear viscoelastic medium. The latter is used to compute consistently V_S and D. The soil is thus assumed to be a dispersive medium and the frequency-dependence is inherently taken into account by the method. Rix and Meng [58], for instance, carried out a N-RC test on a remolded kaolinite sample, showing the "U"-shaped dependence of D_0 from f in a wide range (i.e., 0.01-30Hz) of frequencies (Fig. 4). The results confirmed the trends previously suggested by other Authors (e.g., [55]). The application of the method in the current practice is anyway still limited by the complexity of the approach.

4 In-situ Tests

In situ tests are a common tool for site characterization, due to the limited costs and the rapidity of execution. Moreover, they can provide a reliable estimate of the geotechnical parameters, since they assess the soil behavior in undisturbed conditions at a spatial scale compatible with the geotechnical application of interest.

Geophysical seismic tests are widely-adopted for the determination of G_S on site. On the other hand, some methods have been proposed also for the estimation of D_0. The technical literature also includes some case studies of parameter estimation based on the interpretation of downhole arrays. This approach is less common, as it requires instrumented boreholes with seismic records, but it provides useful data for the assessment of the soil behavior in seismic conditions.

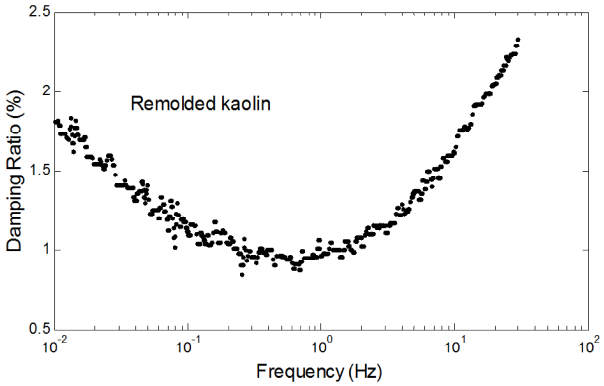

Fig. 4. Dependency of D_0 from f for a remolded kaolinite sample obtained applying the N-RC method (after [58]).

In addition, several seismological studies focus on the attenuation structure of the near-surface. These studies provide an estimate of the dissipation properties in terms of quality factor Q, which is inversely proportional to D_0, on the basis of the high-frequency attenuation of seismic waves. Some of them propose empirical relationships with other geotechnical parameters – e.g., V_S – for specific geological formations. The next sections will focus on the geophysical approaches and the interpretation of borehole arrays.

4.1 Geophysical tests

Geophysical seismic tests are generally classified as invasive and non-invasive. However, all the geophysical methods investigate the medium in its undisturbed natural state, but the sampled soil volume and the resolution are not the same. Therefore, they might provide different results, as a function of the degree of heterogeneity of the soil deposit [80]. There are several interpretation techniques aimed at estimating the small-strain stiffness from the measured data, whereas the attempts of estimating the attenuation characteristics of the soil deposits are less numerous and often restricted to research. Moreover, they sometimes use strong assumptions which limit their applicability. The most important issue is the difficulty in separating geometric and intrinsic attenuation, i.e. the energy loss due to wavefront expansion and to wave scattering in heterogeneous media, on one side, and the one due to intrinsic material attenuation, on the other.

In the following, some applications of the invasive and non-invasive tests for the determination of D_0 are discussed, with focus on their assumptions and limitations.

Invasive tests. Invasive tests are a family of geophysical seismic tests for which a part of the instrumentation is installed in the ground. Typical methods are the Cross-Hole (CH) test [81], Down-Hole (DH) test [82], the P-S suspension logging test, the Seismic Cone Penetration Test (SCPT) [83], the Seismic Dilatometer Test (SDMT) [84] and the direct-push cross-hole test [85]. The technical literature involves many robust approaches for the determination of the shear-wave velocity from the interpretation of the measured data. Conversely, the techniques aimed at estimating the dissipation characteristics of the soil deposit are limited to few attempts with limited applications outside the research field.

Techniques for the estimate of D_0 from CH data are the random decrement approach [86] and the attenuation coefficient method [87-90]. Lai and Özcebe [79] observed that those methodologies rely on the hypothesis of frequency-independent (i.e., hysteretic) damping or on enforcing a specific constitutive model in the interpretation of the attenuation measurements. Moreover, they usually perform an uncoupled estimate of the low-strain parameters by using incompatible constitutive schemes: V_S is obtained according to a linear elastic model, whereas D_0 estimates are based on inelastic models. Therefore, these approaches may lead to inconsistent and biased estimates. To overcome those limitations, they applied the two-station interpretation scheme typical of the SASW method [80] to CH measurements, determining the S wave dispersion function

from the unwrapped phase of the cross-power spectrum $G^{S}_{R_1R_2}$ of the S wave signal, detected at the two receivers.

$$V_S(\omega) = \frac{\omega \Delta L}{arg\, G^{S}_{R_1R_2}} \tag{8}$$

In the equation, the terms R_1 and R_2 denote the distances between each receiver and the source, whereas ΔL is the inter-receiver distance (Fig. 5.a). The procedure then derives D_0 from the computed dispersion curves, by applying the solution of the Kramers-Kronig relation, that relates stiffness and attenuation characteristics in a viscoelastic medium [91].

$$D_0(\omega) = \frac{\frac{2\omega V_S(\omega)}{\pi V_S(0)} \cdot \int_0^{\infty} \left(\frac{V_S(0)}{V_S(\tau)} \cdot \frac{d\tau}{\tau^2 - \omega^2} \right)}{\left[\frac{2\omega V_S(\omega)}{\pi V_S(0)} \cdot \int_0^{\infty} \left(\frac{V_S(0)}{V_S(\tau)} \cdot \frac{d\tau}{\tau^2 - \omega^2} \right) \right]^2 - 1} \tag{9}$$

where $V_S(0) = \lim_{\omega \to 0} V_S(\omega)$.

This interpretation method only requires measurements of velocity for determining either the stiffness or the damping parameters of the material, hence an accurate tracking of particle motions is unnecessary. Moreover, the processing does not require a priori assumptions about the specific rheological behavior or the frequency-dependent nature of D_0. On the other side, broadband seismic sources are required to generate a wave signal with a wide frequency range. If not possible, some assumptions about the dispersive behavior of the soil parameters would be necessary to extrapolate the available data, introducing uncertainties in the estimate (Fig. 5.b).

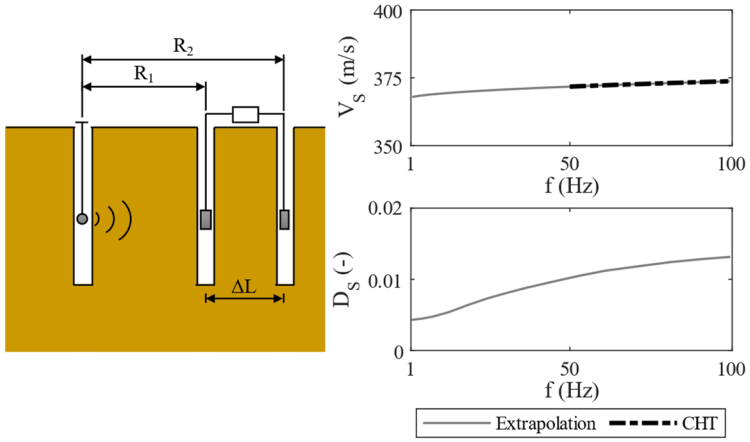

Fig. 5. a) Scheme of the CH test layout; b) resulting dispersion and damping curves from the interpretation of CH data (modified from Lai et al. [79]).

DH and SCPT-based techniques for the estimate of D_0 are theoretically more complex since they should account for the reflection and refraction phenomena at the layer interfaces in the computation of the attenuation. Some interpretation schemes are based on the attenuation coefficient method or on a simulation of the downwards wave propagation in the DH testing. Actually, Stewart and Campanella [92] stated several issues in the application of such approaches, due to the necessity of applying corrections to incorporate the effect of the wave passage through the layer interfaces. Furthermore, the results were affected by large scatter, sometimes providing unphysical values. A popular method is the spectral ratio slope (SRS) method [93; 94]. The approach provides a frequency-dependent estimate of D_0 at depth z_i by computing the 2nd order derivative of the wave amplitude spectral ratio (i.e. the amplitude ratio between the 1st and the ith receiver) with respect to the depth and the frequency.

$$D_0 = \frac{V_S}{2\pi} \cdot \frac{\partial^2}{\partial f \partial z} ln\left(\frac{A_1}{A(z_i)} \right)\Bigg|_{z=z_i} \tag{10}$$

This approach does not require interface corrections and the scatter in the results is low. However, Badsar [95] reported a low reliability of the SRS method in the determination of the damping profile, especially in the presence of complex stratigraphy, due to some simplifying assumptions for the geometrical damping.

A more robust approach is based on the spatial decay of the Arias intensity, developed by Badsar [95]: once determined the V_S profile, the method calibrates the D_0 profile through an optimization algorithm minimizing the difference between the experimental evolution of the Arias intensity among the receivers and the theoretical one, computed for a vertical point force. This method properly considers all the phenomena of reflection and refraction and provides a good estimate of the D_0 profile. On the other side, its application requires an accurate modelling of the V_S profile and long computational time due to the multiple forward analyses.

Non-invasive tests. Non-invasive tests are geophysical seismic tests employing a source and a set of receivers on the ground surface. They include the seismic reflection survey [96], the seismic refraction survey [97], surface wave testing [80] and the horizontal-to-vertical spectral ratio [98]. This section will focus on the techniques based on the measurement of surface waves generated from active sources.

Surface wave methods (SWM) rely on the dispersive behavior of Rayleigh waves in heterogeneous media, for which the phase velocity exhibits a dependence on frequency. Therefore, the procedure consists in acquiring the particle motion, processing the measured data to derive the experimental dispersion relationship and estimating the V_S profile with depth through an inversion scheme, where a theoretical soil model is calibrated to match the experimental data.

The SWM-based estimate of D_0 usually refers to the measurement of the spatial attenuation of surface waves along linear arrays with active sources. This quantity is linked to the geometrical spreading of the Rayleigh waves and the intrinsic dissipation properties of the material. The measurement requires precise tracking of the surface

wave particle motion, since noise and amplitude perturbations might lead to wrong estimates. For this reason, the acquisition setup should guarantee an optimal coupling and verticality of each receiver and a good sensor calibration for uniform response is required [80].

Rix et al. [99] estimated the attenuation curves based on the regression of the displacement amplitude versus offset data, considering the equation for the Rayleigh wave motion due to a harmonic point force [77]. The amplitude-offset regression provides an uncoupled estimate of the dispersion and attenuation curves, which is not mathematically robust and ignores the intrinsic relationship between velocity and attenuation in a linear viscoelastic material [77].

An upgrade of the approach is the transfer function method [100; 101]. The technique is a multistation approach based on the estimate of the experimental displacement transfer function $T(r,\omega)$, i.e. the ratio between the measured vertical displacement at each sensor $u_z(r,\omega)$ with offset *r* and the input harmonic source $F \cdot e^{i\omega t}$ in the frequency domain:

$$T(r,\omega) = \frac{u_z(r,\omega)}{F \cdot e^{i\omega t}} \tag{11}$$

Then, for each frequency, the procedure jointly estimates the complex wavenumber $K(\omega)$ through the nonlinear fitting of the following expression [77]:

$$T(r,\omega) = Y(r,\omega) \cdot e^{-iK(\omega)r} \tag{12}$$

In the equation, $Y(r,\omega)$ is the geometrical spreading function, which is usually assumed as equal to $1/\sqrt{r}$ (e.g., [101; 102]). The complex wavenumber is defined as a combination of the real wavenumber $k(\omega)$ and the attenuation $\alpha(\omega)$, that are linked to the phase velocity and the phase damping of the Rayleigh waves:

$$K(\omega) = k(\omega) - i\alpha(\omega) = \frac{\omega}{V(\omega)} - i\frac{D(\omega)\cdot\omega}{V(\omega)} \tag{13}$$

The fitting of $T(r,\omega)$ can be performed in an uncoupled way, based on the separate fitting of its amplitude and phase [101]. However, a coupled fitting of the transfer function in the complex domain is mathematically more robust and provides an estimate of the wave parameters compatible with amplitude phase data [102] (Fig. 6).

Foti [102; 103] adopted a generalized version of the transfer function method by removing the effect of the input force, whose measurement is nontrivial and requires controlled sources. For this purpose, the Author reformulated the displacement transfer function in terms of deconvolution of the seismic traces. The principle of this method consists in computing the experimental transfer function adopting the response of the closest receiver as the reference trace.

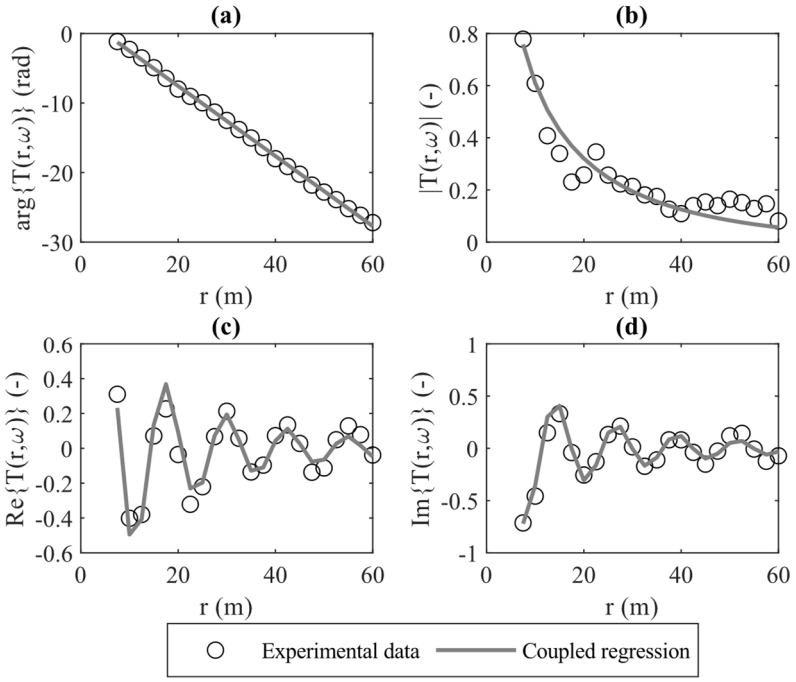

Fig. 6. Regression of the experimental transfer function for the coupled computation of dispersion and attenuation curves: (a) phase; (b) amplitude; (c) real part; (d) imaginary part. The data refer to the Pisa Leaning Tower site, at the frequency 11.5 Hz (modified from Foti [102]).

A limitation of the regression is the assumption that the wavefield is dominated by a single Rayleigh mode of propagation. Therefore, the result is an estimate of apparent Rayleigh phase dispersion and attenuation curves, that can be affected by modal superposition when multiple propagation modes are relevant [80]. For this reason, new advanced methods have been proposed, as the generalized Multiple Signal Classification [104], wavelet decomposition methods [105] or sparse signal reconstruction [106]. Moreover, Badsar et al. [107] proposed a simplified method for the estimate of the attenuation curves, based on a generalization of the half-power bandwidth method, whereas Verachtert et al. [108] introduced an alternative methodology for the determination of multimodal surface wave dispersion curves and attenuation curves, namely the circle fit method.

As for the inversion, a robust characterization method requires a joint inversion of the Rayleigh dispersion and attenuation curves into the V_S and D_0 profiles. The coupled inversion offers the advantages of accounting for the inherent relationships between the stiffness and the attenuation properties in the material and it is a better-posed mathematical problem [101]. Being the inversion procedure commonly based on the solution of multiple forward problems to fit the experimental dispersion and attenuation curves, it requires specific algorithms for the solution of the Rayleigh eigenvalue problem in linear viscoelastic media [101]. Moreover, the coupled inversion requires the definition of a proper misfit function, which should be complex-valued to

incorporate both stiffness and dissipation data. Most of the applications implemented this strategy into a constrained least-squares algorithm, aiming at a smooth profile respecting the experimental data [101-103; 107; 108]. On the other side, there are also some attempts of application of the Monte Carlo technique in the joint inversion for the estimate of the uncertainties [104].

4.2 Back analysis of Down-Hole arrays

Downhole instrumentations for the observation of ground motion represent a valuable tool for understanding the physics of the seismic amplification. The provided data are useful for the validation of theoretical models of amplification, highlighting issues due to the assumptions about the constitutive behavior of the soil deposit (e.g., [10; 13]) or the propagation model (e.g., [46]). Moreover, borehole array data can be employed for the calibration of mechanical parameters by performing a back-calculation from observed ground motions. The literature reports several attempts at estimating the dissipation characteristics from the interpretation of earthquake records in instrumented boreholes (e.g., [109; 110]).

For instance, Assimaki et al. [111; 112] implemented a seismic waveform inversion algorithm for the estimate of the small-strain parameters from weak motion records in downhole arrays. The procedure assumes a 1-D ground model and it estimates the mechanical parameters, i.e. V_S, D_0 and density for each layer, through a two-step optimization algorithm, consisting in a genetic algorithm in the wavelet domain and a nonlinear least-squares in the frequency domain. The stochastic optimization minimizes the misfit between the theoretical and the observed acceleration time histories, represented in the wavelet domain – rather than in the time domain – to ensure equal weighting of the information across all frequency bands. The local search process is a nonlinear least-squares optimization algorithm in the frequency domain, minimizing the error between the theoretical transfer function and the empirical one. The combination of a stochastic search algorithm with a local search one provides the advantages of each technique, resulting in a robust search method.

A quite popular approach of D_0 estimation is based on site-amplification synthetic parameters. The strategy consists in a search procedure where several GRAs are performed by keeping all the other model parameters (V_S, density, layer thickness) constant and iteratively adjusting D_0 to obtain a good level of consistency between the predicted and the observed response. The trial values of D_0 can be assumed a priori [46], on the basis of seismological relationships [113] or from laboratory-based values (e.g., [42]). The resulting value is compatible with the site behavior in seismic conditions and it can be used for GRAs.

The downhole array data processing is not straightforward and it incorporates some drawbacks. On one side, the computation of the empirical site response requires the selection of an adequate number of ground motion histories [112]. The only weak motions should be included, to avoid the rise of nonlinear phenomena and ensure the validity of viscoelastic behavior of the soil deposit [42; 46; 47; 51; 113; 114]. Moreover, a critical issue is the ambiguity about the wavefield conditions at the downhole sensors. Indeed, the downhole sensors record either upgoing or downgoing waves and, due to

the impossibility of separating them, the modelling of their conditions is complex [115]. Finally, the quality of the estimate strongly depends on the reliability of the available geotechnical information and the absence of lateral variabilities [46].

A special remark about the role of the ground motion parameter adopted for measuring the site response should be pointed out. Common descriptors are frequency-domain parameters, as they best carry information about the frequency-dependent phenomenon of site amplification. We might refer to the acceleration transfer function (ATF), i.e. the ratio of the Fourier amplitude spectra between two locations [116], or the amplification function (AF), i.e. the ratio of the elastic response spectra [46]. The description might refer also to time-domain parameters, as the peak values of acceleration and velocity and the Arias intensity [51]. Indeed, they synthesize the ground response of a broad range of frequencies, but the request of matching a time instant parameter might lead to physically unreliable data. An alternative approach adopts the high-frequency spectral attenuation κ_0, which describes the decay of the Fourier amplitude spectrum of the ground motion at high frequencies. The difference of attenuation $\Delta\kappa$ between surface and borehole records provides a measure of the attenuation along the borehole and it is related to the small strain parameters of the soil deposit [117].

$$\Delta\kappa = \int_0^z \frac{2D_0}{V_S} dz \tag{14}$$

In this way, by adjusting the damping parameters, we can identify a κ_0-informed D_0 that suits the observed high-frequency attenuation (e.g., [47; 53; 113]). Fig. 7 shows the effect of the type of parameter on the damping correction for some sites with different geology.

There is no consensus about the best reference parameter. Several case studies performed an estimate in the frequency domain, based on the measured ATF (e.g., [13; 42; 46]). Tao and Rathje [51] suggested keeping the time domain parameters as a reference, since they capture the overall response of the site, whereas the calibration in the frequency domain may lead to an overestimation of the damping. On the other side, Afshari and Stewart [53] stated that the κ_0-informed damping value best fits the observed site response.

5 Literature approaches to account for wave scattering effects

The site characterization, i.e. the procedures and interpretations devoted to the formulation of a geotechnical model, is usually performed through laboratory tests and in situ surveys. Their combined use is strongly recommended by several guidelines, as they are complementary. Indeed, laboratory tests are performed on small-size soil specimens by applying an imposed stress/strain history with known hydro-mechanical boundary conditions, ensuring a controlled behavior and a rigorous estimate of the mechanical

parameters. On the other side, in situ testing does not allow full control of the hydrogeologic and loading conditions, but the investigated soil volume is larger and closer to the representative volume for the geotechnical applications. Moreover, in situ tests are free from effects due to sampling disturbance and also allow the characterization of hard-to-sample soils.

The complementary nature of such tests gives rise to discrepancies between laboratory-based D_0 values and the ones derived from in situ testing or inferred from DH arrays, as highlighted by several studies.

For instance, Foti [102] compared the damping ratio obtained from the SWM and from laboratory testing, observing a slight overestimation of the dissipative properties in the former, due to the presence of additional attenuation mechanisms other than geometric and intrinsic attenuation, especially for shallow layers (Fig. 8).

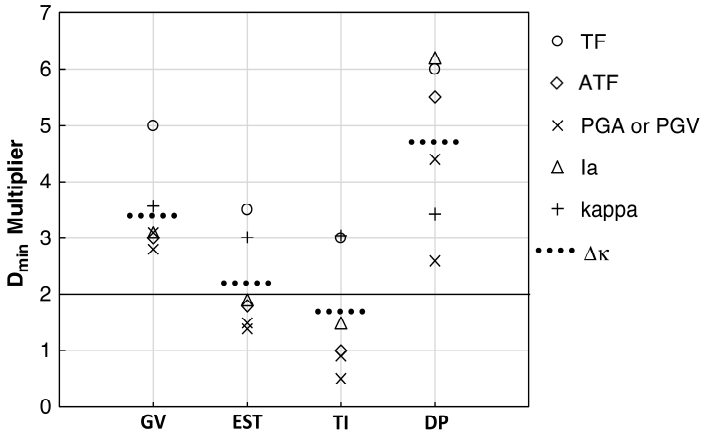

Fig. 7. Obtained damping multipliers for the Garner Valley (GV), EuroSeisTest (EST), Treasure Island (TI) and Delaney Park (DP) sites (after Tao and Rathje [51]).

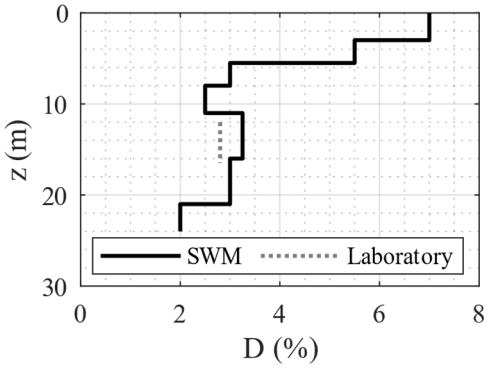

Fig. 8. Comparison between the SWM-based and the laboratory-based damping profile. The data refer to the Pisa Leaning Tower site (modified from Foti [102]).

The numerous studies based on DH arrays highlighted the differences between D_0 and $D_{0,\,site}$. Some preliminary observations about this discrepancy are reported in Tsai and Housner [118] and Dobry et al. [119], where the calibrated $D_{0,\,site}$ was much higher than the intrinsic attenuation properties. The reason for such difference was some bias due to plane wave assumption and the presence of other losses of energy [120]. Recent studies observed high $D_{0,\,site}$ values (either in absolute terms or compared with laboratory data) in soft shallow layers, that usually exhibit strong heterogeneities resulting in relevant scattering phenomena. For instance, Assimaki [111] stated a large increase of the attenuation in the shallow layers due to scattering, that is not accounted in the seismic waveform inversion algorithm, thus resulting in an additional energy loss. Zalachoris and Rathje [42] corrected the D_0 profiles using the ATF-based approach, that led to an increase of the damping ratio ranging between 2% and 5%. They also observed that the incompatibility is strong for deep arrays with no significant impedance contrast, mainly due to the modelled wavefield conditions at the downhole sensors (Fig. 9). Even the κ_0-informed $D_{0,\,site}$ estimate is larger than the laboratory-based D_0, yet still lying close to the upper bounds of the statistical distribution of data. However, some authors questioned the relation between κ_0 and the small strain damping, due to the wave scattering phenomena that may be relevant in the presence of complex stratigraphy [121].

Conversely, Kaklamanos and Bradley [122] observed the necessity of decreasing the laboratory-based D_0, in order to reduce the high-frequency bias of the theoretical model with the observed amplification data. Actually, they recognized the limited physical background of such reduction, justifying it with some breakdowns of the 1-D propagation assumption.

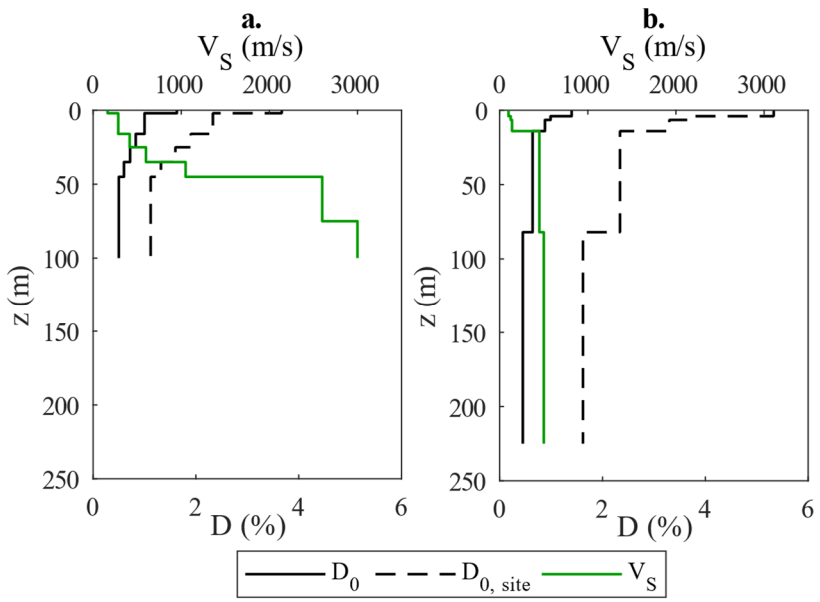

Fig. 9. D_0 profiles and obtained $D_{0,site}$ profiles (dotted line) (a) for a shallow site with a strong impedance contrast and (b) a deep site (modified from Zalachoris and Rathje [42]).

In summary, one of the most important factors affecting the in situ attenuation estimates is the presence of wave scattering phenomena, which is an additional dissipation mechanism not accounted in the laboratory measurements. Seismic wave scattering is a phenomenon characteristic of the wave propagation in heterogeneous media, where the multiple reflections and refractions lead to a non-planar propagation and to the diffusion of the seismic energy.

Generally, the scattering depends on the relative size between the heterogeneity and the wavelength and it holds only when they are compatible [123]. For seismic applications, where the frequency content is close to 1-10 Hz, the material fluctuations usually present in the soil deposits have a significant effect on the wavefield, hence the scattering is a relevant phenomenon [48]. As pointed out by Zalachoris and Rathje [42], the attenuation through wave scattering mechanisms is apparent. Indeed, the energy simply diffuses inside the medium instead of moving only towards the surface, which is perceived as an energy loss on the surface ground motion [123].

The role of wave scattering in the propagation phenomena – hence, in the site response analyses – limits the applicability of GRAs, that rely on the assumption of a planar wave field. For this reason, taxonomic schemes based on DH array data have been proposed to assess whether the 1-D approach is reliable [46; 124]. When the spatial variability of the mechanical parameters is relevant, specific 2-D and 3-D Site Response Analyses (hereafter, SRAs) should be carried out. A common approach is based on generating soil models by assuming the material properties as spatially correlated random fields (e.g., [48]). This approach considers a spatially-correlated statistical distribution of the mechanical parameters, characterized by variance and range, i.e. the distance at which the correlation diminishes. Huang et al. [125] observed that an increase of the variance in the distribution – namely the degree of heterogeneity – induces a reduction of the mean AF, due to the stronger wave scattering in the soil model. The variation in the AF is stronger at high frequencies, as the wavelength is becoming smaller with respect to the size of the heterogeneity. Yet, the performance of 2-D or 3-D analyses requires long computational time and involves a high degree of complexity in the model definition.

An alternative way to mimic lateral heterogeneities and wave scattering phenomena consists in performing a Monte Carlo simulation, by generating multiple 1-D ground models with random V_S realizations and keeping the damping value constant and equal to D_0. Even though it does not explicitly consider lateral variabilities, the average response accounts for the wave scattering that happens in real soil deposits [126]. A classical model for accounting for such variability is the Toro [127] model, that incorporates criteria for the V_S and the layering randomization. Actually, several studies highlighted the limitations of the model (e.g., [5; 51; 128; 129]) and some adjustments in the parameters or even in the framework have been proposed [20]. The V_S randomization mimics the effects of damping at the site natural frequencies. Indeed, the realizations are soil profiles with different fundamental frequencies and the average of the responses results in a smaller and smoother peak. On the other side, it does not have any significant effect on the Fourier amplitude spectrum at high frequencies, hence it does not capture the behavior of κ [51]. Moreover, it does not allow to incorporate

complex phenomena as the presence of surface waves, that introduce additional low-frequency oscillations [130].

6 Influence of D_0 correction in GRAs

A critical step in conducting GRAs is the definition of the soil model and the choice of the parameters. Indeed, the key issue is the non-existence of *a priori* conservative values for the mechanical parameters. For this reason, GRAs should be carried out by considering the parameter uncertainties in an explicit way.

This section shows the influence of the uncertainties in D_0 in the seismic ground amplification, by reporting two case studies.

On one side, we assess the effect of D_0 on a stochastic database of GRAs, which consists of the results of 3,202,500 EQL simulations performed over a collection of 91,500 1-D soil models [131], subjected to seismic inputs of different intensity. In this specific study, we try to map the variations of D_0 on the seismic amplification of a subset of soil models of engineering interest. In this way, we can figure out the role of D_0 on the response of generic soil models under seismic conditions.

On the other side, we assess the influence of D_0 on a site-specific amplification study. For this purpose, we consider the site of Roccafluvione, in the Marche region, which was struck by the seismic sequence that started on the 24th of August 2016. The site was object of intense geological and geotechnical investigations, resulting in a detailed ground model. Foti et al. [19] performed EQL GRAs over a statistical sample of ground models generated through a Monte-Carlo simulation from the results of the investigations, to capture the effects due to the variability in V_S and the MRD curves. In this paper, we analyze the variations in the site response due to changes in the D_0 profile.

In both case studies, the definition of the $D_{0,\,site}$ profile is a nontrivial operation. Indeed, as mentioned previously, there is not a common procedure for its computation. Moreover, no detailed information is available, as there are not DH arrays at the site and no specific geophysical studies for its determination have been carried out. In these conditions, an estimate of $D_{0,\,site}$ can be provided through the procedure prescribed by Stewart et al. [14], who suggested dealing the difference between D_0 and $D_{0,\,site}$ as an epistemic uncertainty. Therefore, for each ground model, we run parallel analyses by assuming different $D_{0,\,site}$ values, given as the sum of D_0 – derived through empirical models – and a depth-independent additional damping ΔD, ranging between zero and 5%. This specific study considered three possible ΔD values: 0% (i.e., $D_{0,\,site}$ coincides with D_0), 2.5% and 5%. The analyses have been performed according to the EQL scheme, with the DEEPSOIL v7.0 software [132; 133].

6.1 Stochastic database of GRAs

Setting of the GRAs. The procedure for the generation of the 1-D ground models consists of a Monte-Carlo simulation, which randomizes a set of real soil profiles and assigns a V_S profile and the MRD curves to each ground model. The extraction of the V_S

profiles with respect to depth is performed by means of a Monte-Carlo procedure, according to the geostatistical model proposed by Passeri [20], which represents an upgrade of the one introduced by Toro [127]. This new model provides a physically-based population of soil models, compatible with the common geological features and the experimental site signatures. Then, the procedure computes the MRD curves derived from the literature models proposed by Darendeli [134], Rollins et al. [135] and Idriss and Sun [136]. The reader can refer to Passeri [20] and Passeri et al. [137] for further details about the model architecture and parameters for V_S profiles generation, whereas information about the MRD curves assignment is available in Aimar et al. [131].

For the sake of simplicity, the study focuses on some groups of profiles of engineering interest. Fig. 10.a shows the investigated regions, represented in the $V_{S,H}$-H domain, that are the time-weighted average of the V_S profile and the thickness of the soil column, respectively. On one side, we include a group of relatively stiff ground models, characterized by $V_{S,H}$ of 400÷450 m/s and bedrock depth close to 50 m, representative of gravelly soil deposits typical of the Alpine valleys (group A). On the other side, we consider three groups of soft soil deposits, with $V_{S,H}$ close to 250 m/s and sediment thickness ranging from 15 m (group B) to 50 m (group C) up to 120 m (group D). These groups represent different possible configurations of alluvial basins. Each set consists of a population of 200 soil models, which can be considered reasonable for statistical purposes. Following the recommendations prescribed in Stewart et al. [14], for each ground model we perform multiple GRAs, by computing $D_{0,\,site}$ as the sum of D_0, derived according to the above-mentioned literature models, and an additional damping ΔD equal to 0%, 2.5% and 5%.

The definition of the seismic input motions refers to two Italian sites, characterized by a small-to-moderate and high level of seismicity. The sites are Termeno sulla Strada del Vino and San Severo, characterized by an expected value of maximum ground acceleration a_g of 0.54 m/s^2 and 2.07 m/s^2, respectively (Fig. 10.b), referred for a return period of 475 years. For each site, 7 natural accelerograms are selected from accredited ground motion databases, in compliance with the criteria of seismological compatibility and spectral compatibility with the reference uniform hazard elastic spectrum [14; 138].

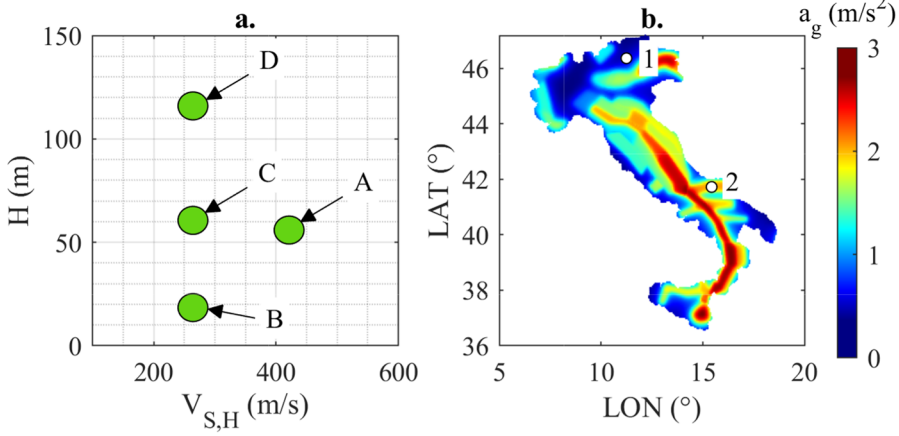

Fig. 10. a) Distribution of the groups of soil deposits in the $V_{S,H}$-H domain; b) position of the reference sites in the Italian seismic hazard map.

Results. For each ground model, results of the GRAs are averaged through logarithmic mean with respect to the input motions, obtaining a representative response for every soil profile under the reference seismicity level. In order to describe the distribution of the results inside each group, the mean and the standard deviation of the spectral ordinates with respect to the ground models are computed, assuming a lognormal distribution of the data [131]. The procedure is applied for the four populations of ground models, for each level of additional damping.

Fig. 11 shows the results in terms of AF for each group of soil models, for low and high seismicity. From the general viewpoint, we can notice that all the soil models exhibit a smaller spectral amplification moving from high frequencies to periods ranging between 0.05 s and 0.2 s. Then, there is a peak at intermediate periods (i.e., 0.5÷1.1 s), corresponding to the average fundamental period of each soil group. These features are enhanced for increasing deformability and depth of the soil deposit. For an increasing level of seismicity, the amplification is smaller and the AF curves shift towards higher vibration periods, due to the rise of nonlinear phenomena.

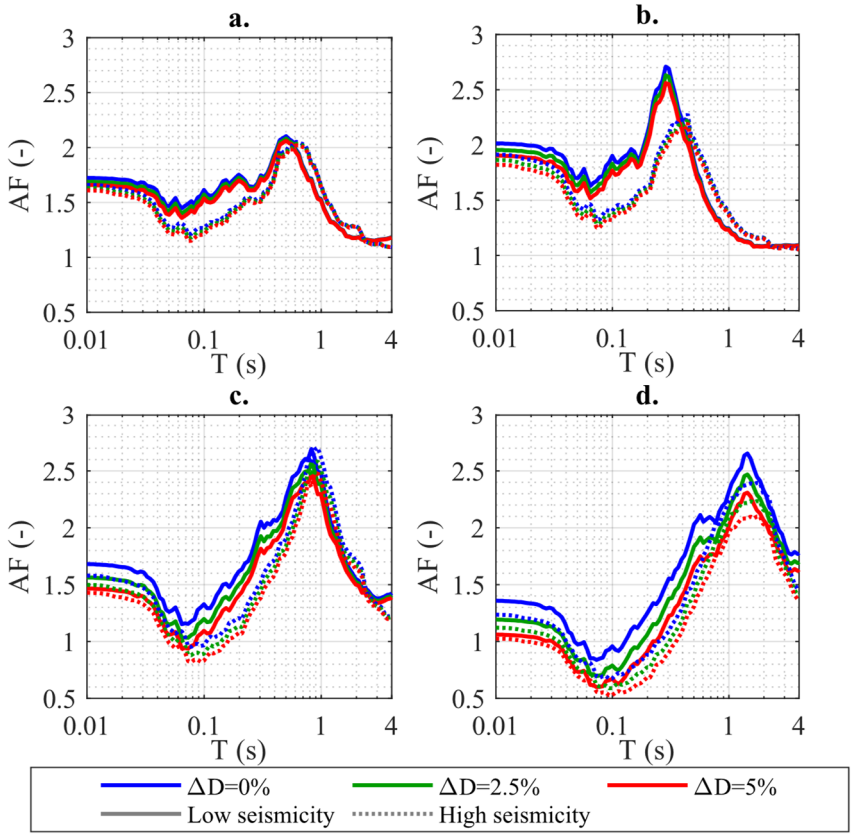

Fig. 11. Mean AFs for groups (a) A, (b) B, (c) C, and (d) D as a function of ΔD and seismicity level.

The impact of $D_{0,\,site}$ depends on the deformability of the ground model and on the level of seismicity. Its increase induces a smaller amplification, but the difference is negligible in shallow soil models (Fig. 11.a-b), with a maximum of 5% at high frequencies and at resonance just in case of soft deposits. This result is consistent with the findings of Stewart and Kwok [7]. Conversely, variations in $D_{0,\,site}$ have a strong influence on the seismic amplification in deep and deformable soil deposits (Fig. 11.c-d). For instance, very deep models undergo a reduction of the AF up to 15% at resonance and 35% at high frequencies for ΔD = 5%. Similar features are observed under strong seismic input motions, even though the effect is less relevant.

As for the variability in the stratigraphic amplification, Fig. 12 shows that it is higher in the range of intermediate periods, exhibiting a narrow peak close to the resonance period in case of shallow soil deposits. The increase of the $D_{0,\,site}$ induces a slight reduction in the variability of AF. This variation is negligible for low deformable soil models, whereas some differences are observed at short vibration periods in soft soil deposits. This kind of ground models, indeed, usually exhibits local variations – i.e., thin layers, in 1-D conditions – that usually induce strong variability in the response.

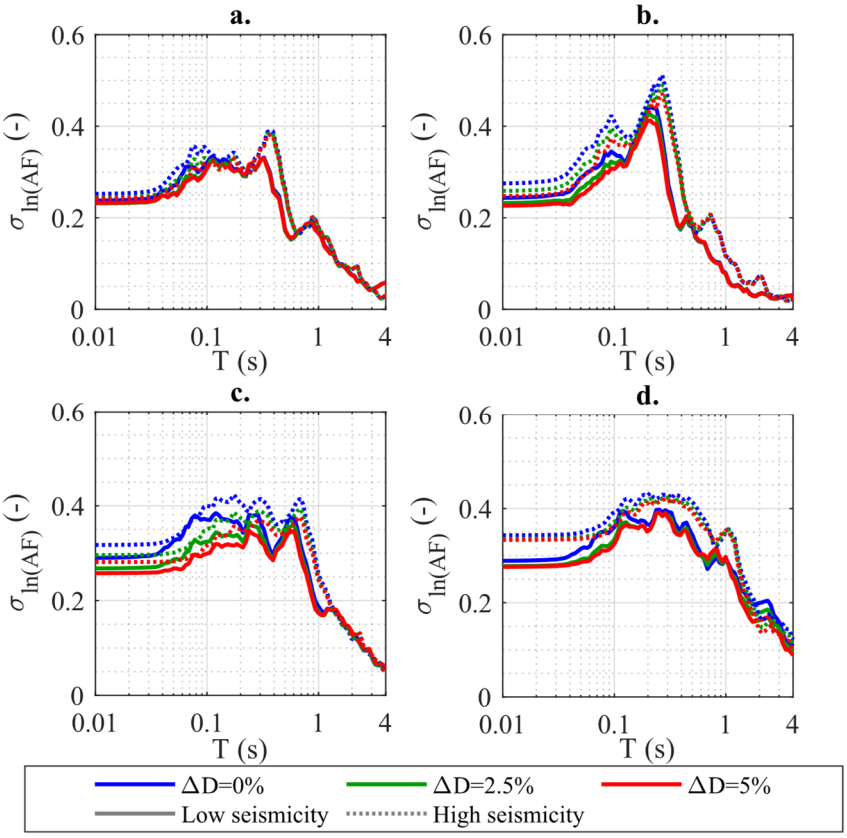

Fig. 12. Standard deviation (in logarithmic scale) of the AFs for groups (a) A, (b) B, (c) C, and (d) D as a function of ΔD and seismicity level.

On the other side, increasing $D_{0,\,site}$ leads to an overdamping of the high-frequency components of the wavefield, that are more sensitive to such variations. Moreover, the effect of $D_{0,\,site}$ on the response variability is observed on soft soil models under strong seismic inputs (e.g., Fig. 12.c). A possible reason might be the shifting of the D curve towards higher values at large strains due to the increase of $D_{0,\,site}$, resulting in an additional attenuation of the high-frequency components of the wave.

6.2 The Roccafluvione Case-Study

Setting of the GRAs. The stratigraphy of the Roccafluvione site is characterized by a 25 m-thick stratification of silty sands, lying over a formation of sands and gravels. A MASW survey provided an estimate of the V_S profile, shown in Fig. 13.a. The study adopts the MRD curves proposed by Ciancimino et al. [38], which is a specialized version of the Darendeli [33] model, adapted to capture the specific behaviour of silty and clayey soils from the Central Italy area. More details about the stratigraphy and the parameter computation are available in Foti et al. [139].

The uncertainties of $D_{0,\,site}$ are simulated through the approach suggested by Stewart et al. [14]. More specifically, the study focuses on three soil models characterized by the V_S profile shown in Fig. 13.a and $D_{0,\,site}$ computed as the sum of D_0 and an additional contribution ΔD, equal to 0%, 2.5% and 5%. The D_0 value is computed according to the model proposed by Ciancimino et al. [38], for a reference frequency of 1 Hz in order to account for the rate-dependence of this parameter.

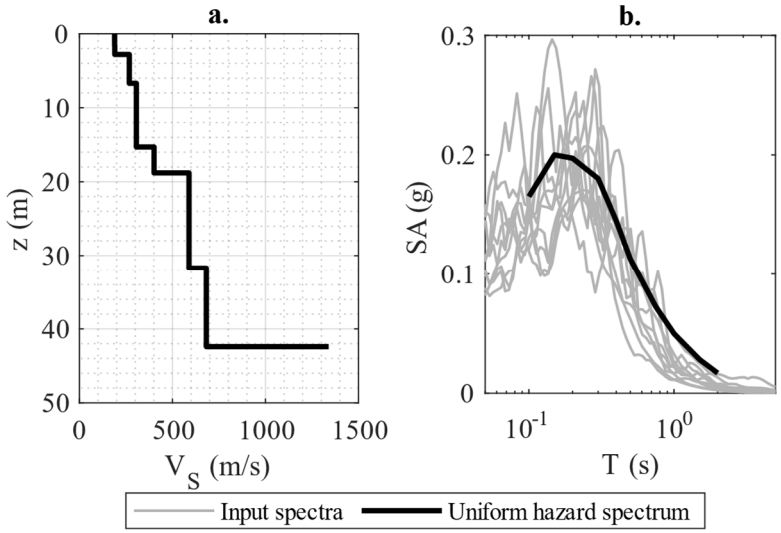

Fig. 13. a) V_S profile obtained from the MASW survey; b) comparison between the elastic response spectra of the input motions and the uniform hazard spectrum, for the return period of 50 years.

The input motions consist of unscaled seismologically and spectrum-compatible acceleration time histories, selected from accredited strong-motion databases. The reference hazard levels correspond to the target Uniform Hazard Spectra for the return period of 50 and 475 years, provided by the National Institute of Geophysics and Volcanology (INGV) [140] (Fig. 13.b). For each reference return period, ten time histories are selected.

Results. For each ground model, results are averaged through logarithmic mean with respect to the input motions, obtaining a representative response for every soil profile under the reference ground motion.

Fig. 14 shows the AFs for each ground model for the weak motions (Fig. 14.a) and the strong motions (Fig. 14.b). The models exhibit a large amplification of the spectral ordinates for a wide range of vibration periods, especially at short periods and close to 0.25 s, which is the fundamental period of the soil deposit.

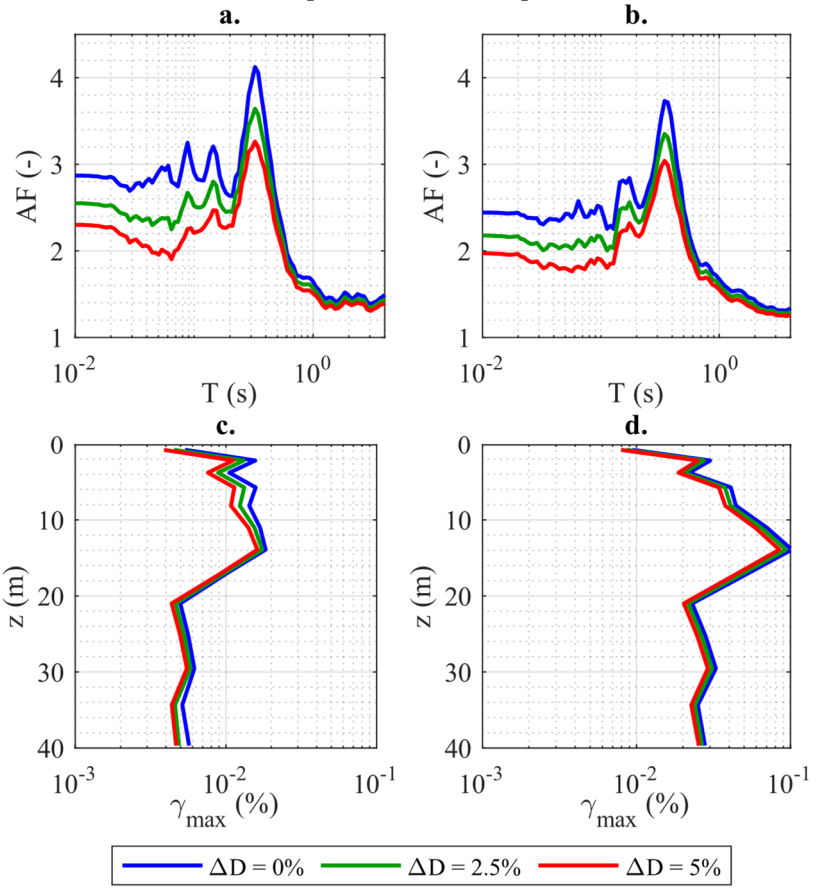

Fig. 14. Mean AFs as a function of ΔD, for (a) the reference return period of 50 years and (b) 475 years; maximum strain profiles for an input motion as a function of ΔD, for (c) the reference return period of 50 years and (d) 475 years.

The effect of the variations in $D_{0,\,site}$ results in a deviation between the curves: for increasing dissipative properties, AF is smaller and the peaks are smoother. This effect is strong for short vibration periods, as the dissipative properties mainly affect the high-frequency components of the propagating wave, and at the resonance peak. For long vibration periods, the role of ΔD is negligible. When the seismicity level is higher, the role of $D_{0,\,site}$ is less significant, as the variation in terms of AF is smaller. Indeed, the maximum strain level increases of about one order of magnitude in all the ground model and the peak value shifts from 2×10^{-2}% to 10^{-1}%, as shown in Fig. 14.c-d. Therefore, the nonlinear behavior strongly influences the response of the soil deposit and the small-strain parameters are less important.

It is interesting to compare the variations in the AF due to the epistemic uncertainty in the small-strain damping with the variability due to V_S and the MRD curves. Such variability was computed by keeping $D_{0,\,site}$ as equal to D_0 in Foti et al. [139], resulting in a distribution of AF represented by the interval defined by the mean and one standard deviation (in logarithmic scale) in Fig. 15.a-b. By overlapping the curves obtained as a function of ΔD with the AF distribution, we notice that a change in $D_{0,site}$ leads to a variation in the amplification which is not negligible if compared with the overall variability of the results. Indeed, for ΔD = 2.5%, the AF is close to the lower boundary of the distribution, whereas a value ΔD = 5% leads to a large reduction of the amplification, which lies completely below the bounds. This effect is relevant especially at high frequencies and close to the resonance peak. This difference demonstrates than variations in $D_{0,\,site}$ may have an impact as strong as the ones in V_S and the MRD curves and its proper quantification is necessary for a good prediction of the ground response in seismic conditions.

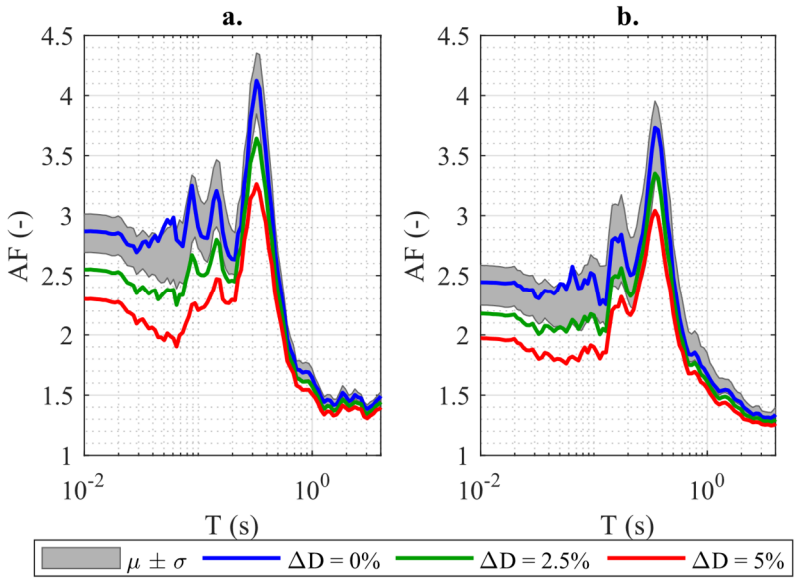

Fig. 15. Comparison between the AF distribution obtained by varying V_S and the MRD curves and the AF curves as function of ΔD for (a) the reference return period of 50 years and (b) 475 years.

7 Final Remarks

The small-strain damping, along with the V_S profile, governs the response of a site in the almost linear range of the stress-strain behavior. Specifically, it affects the amplitude of the amplification functions.

In the present paper, the critical issues associated to the determination of the small-strain damping were firstly treated. Several tests can be carried out to measure the soil damping, either in laboratory or *in situ* through specific geophysical investigations. Each test is of course characterized by different advantages and disadvantages which may affect the measured values, but besides the differences a main bias emerges: the small-strain damping observed in field is usually higher with respect to the one measured in laboratory. These differences are generally attributed to wave scattering mechanisms that cannot be captured by laboratory tests. This bias affects the overall site response. A GRA performed neglecting wave scattering phenomena will in fact lead in an overestimation of the seismic motion at the surface, as shown by the comparisons of GRAs results with the actual motions measured by borehole arrays.

Although these differences are nowadays well-recognized, the difficulties associated with the determination of $D_{0,\,site}$ lead, usually, to the adoption of laboratory-based values, neglecting wave scattering phenomena. Moreover, the uncertainties associated to the small-strain damping are generally thought to be less relevant when compared, for instance, to the variability coming from the V_S profile and the MRD curves, especially when soil nonlinearity is involved.

A stochastic database of GRAs was then used in the present study to assess the actual influence of the small-strain damping on the seismic amplification. The study involved four different groups of 200 soil profiles subjected to seismic inputs of different intensity. Each group corresponds to a specific range of $V_{S,H}$ and bedrock depth. In order to study the influence of wave scattering phenomena, for each ground model multiple GRAs were performed by computing $D_{0,\,site}$ as the sum of laboratory-based D_0 and a ΔD, assumed to be equal to 0%, 2.5% and 5%. The results show a moderate impact of the small-strain damping. The differences start anyway to be relevant when deep and deformable models are considered. For these models, a reduction of the average amplification function is observed up to 15% at resonance and to 35% at high frequencies, when ΔD is assumed to be 5%.

Subsequently, the influence of D_0 on a specific case-study was assessed by considering the well-documented Roccafluvione site. Different input motions were selected to match the Uniform Hazard Spectra of the site for the return periods of 50 and 475 years. A considerable impact of the small-strain damping was observed even when the soil profile is subjected to the higher seismicity level. For an increasing level of ΔD the amplification functions get significantly reduced and the peaks become smoother. The variability coming from ΔD was then compared to the range of amplification functions defined considering the uncertainties related to MRD curves and V_S profile of the site. At least for this specific situation, ΔD seems to be even more relevant with respect to the uncertainties in the other parameters. The amplification function at high frequencies falls in fact outside the range previously defined when at least a ΔD of 2.5% is taken into account. The role of ΔD becomes negligible just for periods higher than 0.5s.

It is quite evident that the differences between site and laboratory values of the damping cannot be *a priori* neglected. The uncertainties related to D_0 have in fact proven to be relevant in specific situations, leading to a modification of the expected ground motion at the surface. At the current state of practice anyway, there are not effective methods to take into account the differences between laboratory and site values of D_0. More efforts should then be devoted to improving our knowledge on the topic in order to develop specific and effective tools to manage the uncertainties related to the small-strain damping.

Acknowledgements

Special thanks to Dr Federico Passeri, for letting us use his procedure of generation of soil profiles and for his cooperation on the subject of this paper. The study has been partially supported by the ReLUIS project, funded by the Italian Civil Protection Agency.

References

1. Seed H.B., Idriss I.M.: Ground motions and soil liquefaction during earthquakes. Earthquake engineering research insititute: (1982).
2. Aki K.: Local site effects on weak and strong ground motion. Tectonophysics 218 (1-3): 93-111 (1993).
3. Kramer S.L.: Geotechnical earthquake engineering. International series in civil engineering and engineering mechanics. New Jersey, (1996).
4. Olsen K.: Site amplification in the Los Angeles basin from three-dimensional modeling of ground motion. Bulletin of the Seismological Society of America 90 (6B): S77-S94 (2000).
5. Rodriguez-Marek A., Rathje E., Bommer J., Scherbaum F., Stafford P.: Application of single-station sigma and site-response characterization in a probabilistic seismic-hazard analysis for a new nuclear site. Bulletin of the Seismological Society of America 104 (4): 1601-1619 (2014).
6. Faccioli E., Paolucci R., Vanini M.: Evaluation of probabilistic site-specific seismic-hazard methods and associated uncertainties, with applications in the Po Plain, northern Italy. Bulletin of the Seismological Society of America 105: 2787-2807 (2015).
7. Stewart J.P., Kwok A.O.L.: Nonlinear seismic ground response analysis: Code usage protocols and verification against vertical array data. Geotechnical earthquake engineering and soil dynamics IV. (2008).
8. Baturay M.B., Stewart J.P.: Uncertainty and bias in ground-motion estimates from ground response analyses. Bulletin of the Seismological Society of America 93: 2025-2042 (2003).
9. Asimaki D., Li W., Steidl J., Schmedes J.: Quantifying nonlinearity susceptibility via site-response modeling uncertainty at three sites in the Los Angeles Basin. Bulletin of the Seismological Society of America 98 (5): 2364-2390 (2008).

10. Kwok A.O.L., Stewart J.P., Hashash Y.M.A.: Nonlinear ground-response analysis of Turkey Flat shallow stiff-soil site to strong ground motion. Bulletin of the Seismological Society of America 98: 331-343 (2008).
11. Li W., Asimaki D.: Site-and motion-dependent parametric uncertainty of site-response analyses in earthquake simulations. Bulletin of the Seismological Society of America 100: 954-968 (2010).
12. Asimaki D., Li W.: Site-and ground motion-dependent nonlinear effects in seismological model predictions. Soil Dynamics and Earthquake Engineering 32: 143-151 (2012).
13. Kaklamanos J., Bradley B.A., Thompson E.M., Baise L.G.: Critical parameters affecting bias and variability in site-response analyses using KiK-net downhole array data. Bulletin of the Seismological Society of America 103: 1733-1749 (2013).
14. Stewart J.P., Afshari K., Hashash Y.M.A.: Guidelines for performing hazard-consistent one-dimensional ground response analysis for ground motion prediction. In: PEER Report 2014, 2014.
15. Kaklamanos J., Baise L.G., Thompson E.M., Dorfmann L.: Comparison of 1D linear, equivalent-linear, and nonlinear site response models at six KiK-net validation sites. Soil Dynamics and Earthquake Engineering 69: 207-219 (2015).
16. Seed H., Idriss I.: Soil moduli and damping factors for dynamic response analyses, Report no. EERC 70-10. Earthquake Engineering Research Center, University of California, Berkeley, California: (1970).
17. Anderson D.G., Woods R.D.: Comparison of field and laboratory shear moduli. In: In Situ Measurement of Soil Properties, Raleigh, N.C., 1975. ASCE, pp 66-92
18. Stokoe K., Santamarina J.C.: Seismic-wave-based testing in geotechnical engineering. In: ISRM International Symposium, 2000. International Society for Rock Mechanics,
19. Foti S., Passeri F., Rodriguez-Marek A.: Uncertainties and variabilities in seismic ground response analyses. In: Earthquake Geotechnical Engineering for Protection and Development of Environment and Constructions: Proceedings of the 7th International Conference on Earthquake Geotechnical Engineering,(ICEGE 2019), June 17-20, 2019, Rome, Italy, 2019. CRC Press, p 153
20. Passeri F.: Development of an advanced geostatistical model for shear wave velocity profiles to manage uncertainties and variabilities in Ground Response Analyses. Ph. D. dissertation, Politecnico di Torino, (2019).
21. Idriss I.M.: Evolution of the state of practice. International Workshop on the Uncertainties in Nonlinear Soil Properties and Their Impact on Modeling Dynamic Soil Response. Pacific Earthquake Engineering Research Center Richmond, Calif., (2004).
22. Rathje E.M., Kottke A.R., Trent W.L.: Influence of input motion and site property variabilities on seismic site response analysis. Journal of geotechnical and geoenvironmental engineering 136: 607-619 (2010).
23. Schnabel PB L.J., Seed HB: SHAKE: A computer program for earthquake response analysis of horizontally layered sites. , vol 72-12. University of California, Berkeley, CA (1972).
24. Matasovic N., Hashash Y.: Practices and procedures for site-specific evaluations of earthquake ground motions. vol Project 20-05 (Topic 42-03). (2012).
25. Kim B., Hashash Y.M.A., Stewart J.P., Rathje E.M., Harmon J.A., Musgrove M.I., Campbell K.W., Silva W.J.: Relative differences between nonlinear and equivalent-linear 1-D site response analyses. Earthquake Spectra 32: 1845-1865 (2016).

26. Hashash Y., Phillips C., Groholski D.R.: Recent advances in non-linear site response analysis. Paper presented at the Fifth International Conferences on Recent Advances in Geotechnical Earthquake Engineering and Soil Dynamics., San Diego, California (2010).
27. Régnier J., Bonilla L.F., Bard P.Y., Bertrand E., Hollender F., Kawase H., Sicilia D., Arduino P., Amorosi A., Asimaki D.: PRENOLIN: International benchmark on 1D nonlinear site-response analysis—Validation phase exercise. Bulletin of the Seismological Society of America 108 (2): 876-900 (2018).
28. Hardin B.O., Drnevich V.P.: Shear modulus and damping in soils: design equations and curves. Journal of Soil Mechanics & Foundations Div 98 (7): 667-692 (1972).
29. Kokusho T., Yoshida Y., Esashi Y.: Dynamic properties of soft clay for wide strain range. Soils and Foundations 22 (4): 1-18 (1982).
30. Seed H.B., Wong R.T., Idriss I., Tokimatsu K.: Moduli and damping factors for dynamic analyses of cohesionless soils. Journal of geotechnical engineering 112 (11): 1016-1032 (1986).
31. Vucetic M., Dobry R.: Effect of soil plasticity on cyclic response. Journal of geotechnical engineering 117 (1): 89-107 (1991).
32. Ishibashi I., Zhang X.: Unified dynamic shear moduli and damping ratios of sand and clay. Soils and Foundations 33 (1): 182-191 (1993).
33. Darendeli M.B.: Development of a new family of normalized modulus reduction and material damping curves. PhD Dissertation, University of Texas at Austin, (2001).
34. Menq F.-y.: Dynamic properties of sandy and gravelly soils. University of Texas, Austin, USA, (2003).
35. Zhang J., Andrus R.D., Juang C.H.: Normalized shear modulus and material damping ratio relationships. Journal of Geotechnical and Geoenvironmental Engineering 131 (4): 453-464 (2005).
36. Senetakis K., Anastasiadis A., Pitilakis K.: Normalized shear modulus reduction and damping ratio curves of quartz sand and rhyolitic crushed rock. Soils and Foundations 53 (6): 879-893 (2013).
37. Vardanega P., Bolton M.: Stiffness of clays and silts: Normalizing shear modulus and shear strain. Journal of Geotechnical and Geoenvironmental Engineering 139 (9): 1575-1589 (2013).
38. Ciancimino A., Lanzo G., Alleanza G.A., Amoroso S., Bardotti R., Biondi G., Cascone E., Castelli F., Di Giulio A., d' Onofrio A., Foti S., Lentini V., Madiai C., Vessia G.: Dynamic characterization of fine-grained soils in Central Italy by laboratory testing. Bulletin of Earthquake Engineering (S.I. : SEISMIC MICROZONATION OF CENTRAL ITALY): 29. doi:https://doi.org/10.1007/s10518-019-00611-6 (2019).
39. Akeju O.V., Senetakis K., Wang Y.: Bayesian Parameter Identification and Model Selection for Normalized Modulus Reduction Curves of Soils. Journal of Earthquake Engineering: 1-29 (2017).
40. Park D., Hashash Y.M.: Evaluation of seismic site factors in the Mississippi Embayment. II. Probabilistic seismic hazard analysis with nonlinear site effects. Soil Dynamics and Earthquake Engineering 25 (2): 145-156 (2005).
41. Yee E., Stewart J.P., Tokimatsu K.: Elastic and large-strain nonlinear seismic site response from analysis of vertical array recordings. Journal of Geotechnical and Geoenvironmental Engineering 139 (10): 1789-1801 (2013).

42. Zalachoris G., Rathje E.M.: Evaluation of one-dimensional site response techniques using borehole arrays. Journal of Geotechnical and Geoenvironmental Engineering 141 (12): 04015053 (2015).
43. Shi J., Asimaki D.: From stiffness to strength: Formulation and validation of a hybrid hyperbolic nonlinear soil model for site-response analyses. Bulletin of the Seismological Society of America 107 (3): 1336-1355 (2017).
44. Cornell C.A.: Engineering seismic risk analysis. Bulletin of the seismological society of America 58: 1583-1606 (1968).
45. Passeri F., Bahrampouri M., Rodriguez-Marek A., Foti S.: Influence of the Uncertainty in Bedrock Characteristics on Seismic Hazard: A Case Study in Italy. Paper presented at the Geotechnical Earthquake Engineering and Soil Dynamics V, (2018).
46. Thompson E.M., Baise L.G., Tanaka Y., Kayen R.E.: A taxonomy of site response complexity. Soil Dynamics and Earthquake Engineering 41: 32-43 (2012).
47. Xu B., Rathje E.M., Hashash Y., Stewart J., Campbell K., Silva W.J.: κ 0 for Soil Sites: Observations from Kik-net Sites and Their Use in Constraining Small-Strain Damping Profiles for Site Response Analysis. Earthquake Spectra (2019): 0000-0000 (2019).
48. Thompson E.M., Baise L.G., Kayen R.E., Guzina B.B.: Impediments to predicting site response: Seismic property estimation and modeling simplifications. Bulletin of the Seismological Society of America 99 (5): 2927-2949 (2009).
49. Field E.H., Jacob K.H.: Monte-Carlo simulation of the theoretical site response variability at Turkey Flat, California, given the uncertainty in the geotechnically derived input parameters. Earthquake Spectra 9: 669-701 (1993).
50. Cabas A., Rodriguez-Marek A. (2018) Toward Improving Damping Characterization for Site Response Analysis. In: Geotechnical Earthquake Engineering and Soil Dynamics V: Seismic Hazard Analysis, Earthquake Ground Motions, and Regional-Scale Assessment. American Society of Civil Engineers Reston, VA, pp 648-657
51. Tao Y., Rathje E.M.: Insights into Modeling Small-Strain Site Response Derived from Downhole Array Data. Journal of Geotechnical and Geoenvironmental Engineering 145 (7): 04019023 (2019).
52. Boaga J., Renzi S., Deiana R., Cassiani G.: Soil damping influence on seismic ground response: A parametric analysis for weak to moderate ground motion. Soil Dynamics and Earthquake Engineering 79: 71-79 (2015).
53. Afshari K., Stewart J.P.: Insights from California Vertical Arrays on the Effectiveness of Ground Response Analysis with Alternative Damping Models. Bulletin of the Seismological Society of America 109 (4): 1250-1264 (2019).
54. Shibuya S., Mitachi T., Fukuda F., Degoshi T.: Strain rate effects on shear modulus and damping of normally consolidated clay. Geotechnical testing journal 18 (3): 365-375 (1995).
55. d'Onofrio A., Silvestri F., Vinale F.: Strain rate dependent behaviour of a natural stiff clay. Soils and Foundations 39 (2): 69-82 (1999).
56. Stokoe K., Darendeli M., Andrus R., Brown L.: Dynamic soil properties: laboratory, field and correlation studies. In: 2nd International Conference of Earthquake Geotechnical Engineering, 1999. pp 811-846
57. Matešić L., Vucetic M.: Strain-rate effect on soil secant shear modulus at small cyclic strains. Journal of geotechnical and geoenvironmental engineering 129 (6): 536-549 (2003).

58. Rix G.J., Meng J.: A non-resonance method for measuring dynamic soil properties. Geotechnical Testing Journal 28 (1): 1-8 (2005).
59. ASTM D4015–15e1: Standard Test Methods for Modulus and Damping of Soils by Fixed-Base Resonant Column Devices. American Society for Testing Material, West Conshohocken, Pennsylvania (2015).
60. Isenhower W.M.: Torsional simple shear/resonant column properties of San Francisco Bay mud. University of Texas at Austin, (1979).
61. Richart F.E., Hall J.R., Woods R.D.: Vibrations of soils and foundations. (1970).
62. Kim D.S.: Deformational characteristics of soils at small to intermediate strains from cyclic test. PhD dissertation, University of Texas at Austin, (1991).
63. Hwang S.K.: Dynamic properties of natural soils. PhD Dissertation, University of Texas at Austin, (1997).
64. Cascante G., Vanderkooy J., Chung W.: Difference between current and voltage measurements in resonant-column testing. Canadian Geotechnical Journal 40 (4): 806-820 (2003).
65. Wang Y.-H., Cascante G., Santamarina J.C.: Resonant column testing: the inherent counter emf effect. Geotechnical Testing Journal 26 (3): 342-352 (2003).
66. Meng J., Rix G.: Reduction of equipment-generated damping in resonant column measurements. Géotechnique 53 (5): 503-512 (2003).
67. ASTM D5311/D5311M–13: Standard Test Method for Load Controlled Cyclic Triaxial Strength of Soil. Amer, West Conshohocken, Pennsylvania (2013).
68. ASTM D3999/D3999M-11e1: Standard Test Methods for the Determination of the Modulus and Damping Properties of Soils Using the Cyclic Triaxial Apparatus. American Society for Testing Material, West Conshohocken, Pennsylvania (2011).
69. Burland J., Symes M.: A simple axial displacement gauge for use in the triaxial apparatus. Geotechnique 32 (1): 62-65 (1982).
70. Ladd R.S., Dutko P.: Small Strain Measurements Using Triaxial Apparatus. In: Advances in the Art of Testing Soils Under Cyclic Conditions, 1985. ASCE, pp 148-165
71. Goto S., Tatsuoka F., Shibuya S., Kim Y., Sato T.: A simple gauge for local small strain measurements in the laboratory. Soils and foundations 31 (1): 169-180 (1991).
72. Doroudian M., Vucetic M.: A direct simple shear device for measuring small-strain behavior. Geotechnical Testing Journal 18 (1): 69-85 (1995).
73. Bjerrum L., Landva A.: Direct simple-shear tests on a Norwegian quick clay. Geotechnique 16 (1): 1-20 (1966).
74. Doroudian M., Vucetic M.: Small-strain testing in an NGI-type direct simple shear device. In: Proc. 11th Danube-European Conf. on Soil Mechanics and Geotech. Engrg., Porec, Croatia, AA Balkema, 1998. pp 687-693
75. Park D., Hashash Y.M.: Rate-dependent soil behavior in seismic site response analysis. Canadian Geotechnical Journal 45 (4): 454-469 (2008).
76. Kim D.-s., Stokoe K.: Torsional motion monitoring system for Small-Strain (10− 5 to 10− 3%) soil testing. Geotechnical Testing Journal 17 (1): 17-26 (1994).
77. Lai C.G., Rix G.J.: Simultaneous inversion of Rayleigh phase velocity and attenuation for near-surface site characterization. (1998).

78. Lai C., Pallara O., Presti D.L., Turco E. (2001) Low-strain stiffness and material damping ratio coupling in soils. In: Advanced Laboratory Stress-Strain Testing of Geomaterials. Routledge, pp 265-274
79. Lai C., Özcebe A.: Non-conventional methods for measuring dynamic properties of geomaterials. In: 6th International Conference on Earthquake Geotechnical Engineering. Christchurch, New Zealand, 2015.
80. Foti S., Lai C., Rix G.J., Strobbia C.: Surface wave methods for near-surface site characterization. CRC press, (2014).
81. ASTM D4428/D4428M-14: Standard Test Methods for Cross-hole Seismic Testing. American Society for Testing Material, West Conshohocken, Pennsylvania (2014).
82. ASTM D7400-17: Standard Test Methods for Downhole Seismic Testing. American Society for Testing Material, West Conshohocken, Pennsylvania (2017).
83. Campanella R.G. (1994) Field methods for dynamic geotechnical testing: An overview of capabilities and needs. In: Dynamic Geotechnical Testing II. ASTM International,
84. Marchetti S., Monaco P., Totani G., Marchetti D.: In situ tests by seismic dilatometer. In: Symposium Honoring Dr. John H. Schmertmann for His Contributions to Civil Engineering at Research to Practice in Geotechnical Engineering, New Orleans, Louisiana, US, 2008.
85. Cox B.R., Stolte A.C., Stokoe II K.H., Wotherspoon L.M.: A direct-push crosshole test method for the in-situ evaluation of high-resolution P-and S-wave velocity. Geotechnical Testing Journal 42: (2018).
86. Aggour M., Yang J., Al-Sanad H.: Application of the random decrement technique in the determination of damping of soils. In: European conference on earthquake engineering. 7, 1982. pp 337-344
87. Hoar R.J., Stokoe K.H.: Field and laboratory measurements of material damping of soil in shear. In: 8th World Conference on Earthquake Engineering, San Francisco, 1984. pp 47-54
88. Mok Y.J., Sanchez-Salinero I., Stokoe K.H., Roesset J.M.: In situ damping measurements by crosshole seismic method. In: Earthquake Engineering and Soil Dynamics II - Recent Advances in Ground-Motion Evaluation, Park City, Utah, US, 1988. vol n. pp 305-320
89. Michaels P.: In situ determination of soil stiffness and damping. Journal of Geotechnical and Geoenvironmental Engineering 124 (8): 709-719 (1998).
90. Hall L., Bodare A.: Analyses of the cross-hole method for determining shear wave velocities and damping ratios. Soil Dynamics and Earthquake Engineering 20 (1-4): 167-175 (2000).
91. Christensen R.: Theory of viscoelasticity: an introduction. Elsevier, (2012).
92. Campanella R.G., Stewart W.P.: Downhole seismic cone analysis using digital signal processing. In: Second International Conference on Recent Advances in Geotechnical Earthquake Engineering and Soil Dynamics, Saint Louis, Missouri, US, 1991. pp 77-82
93. Redpath B.B., Edwards R.B., Hale R.J., Kintzer F.C.: Development of field techniques to measure damping values for near-surface rocks and soils. NSF (1982).
94. Crow H., Hunter J.A., Motazedian D.: Monofrequency in situ damping measurements in Ottawa area soft soils. Soil Dynamics and Earthquake Engineering 31 (12): 1669-1677 (2011).
95. Badsar S.: In-Situ Determination of Material Damping in the Soil at Small Deformation Ratios (In situ bepaling van de materiaaldemping in de grond bij kleine vervormingen). KU Leuven, (2012).

96. Schepers R.: A seismic reflection method for solving engineering problems. Journal of Geophysics: (1975).
97. International A.: Standard Guide for Using the Seismic Refraction Method for Subsurface Investigation—ASTM D5777. ASTM International, (2011).
98. Bard P.Y., SESAME Participants: The SESAME project: an overview and main results. In: 13th World Conference on Earthquake Engineering, Vancouver, BC, Canada, , 2004. pp 1-6
99. Rix G.J., Lai C.G., Wesley Spang Jr. A.: In situ measurement of damping ratio using surface waves. Journal of Geotechnical and Geoenvironmental Engineering 126 (5): 472-480 (2000).
100. Rix G.J., Lai C.G., Foti S.: Simultaneous measurement of surface wave dispersion and attenuation curves. Geotechnical Testing Journal 24 (4): 350-358 (2001).
101. Lai C.G., Rix G.J., Foti S., Roma V.: Simultaneous measurement and inversion of surface wave dispersion and attenuation curves. Soil Dynamics and Earthquake Engineering 22 (9-12): 923-930 (2002).
102. Foti S.: Small-strain stiffness and damping ratio of Pisa clay from surface wave tests. Geotechnique 53 (5): 455-461 (2003).
103. Foti S.: Using transfer function for estimating dissipative properties of soils from surface-wave data. Near Surface Geophysics 2 (4): 231-240 (2004).
104. Misbah A.S., Strobbia C.L.: Joint estimation of modal attenuation and velocity from multichannel surface wave data. Geophysics 79 (3): EN25-EN38 (2014).
105. Bergamo P., Maranò S., Imperatori W., Fäh D.: Wavedec code: an application to the joint estimation of shear modulus and dissipative properties of the near-surface from multi-component, active surface-wave surveys. In: 36th General Assembly of the European Seismological Commission, ESC2018, Valletta, Malta, 2018.
106. Mun S.-C., Zeng S.-S.: Estimation of Rayleigh wave modal attenuation from near-field seismic data using sparse signal reconstructions. Soil Dynamics and Earthquake Engineering 107: 1-8 (2018).
107. Badsar S.A., Schevenels M., Haegeman W., Degrande G.: Determination of the material damping ratio in the soil from SASW tests using the half-power bandwidth method. Geophysical Journal International 182 (3): 1493-1508 (2010).
108. Verachtert R., Lombaert G., Degrande G.: Multimodal determination of Rayleigh dispersion and attenuation curves using the circle fit method. Geophysical Journal International 212 (3): 2143-2158 (2017).
109. Shima E.: Modifications of seismic waves in superficial soil layers as verified by comparative observations on and beneath the surface. Bulletin of the Earthquake Research Institute 40: 187-259 (1962).
110. Pecker A.: Validation of small strain properties from recorded weak seismic motions. Soil Dynamics and Earthquake Engineering 14 (6): 399-408 (1995).
111. Assimaki D., Steidl J., Liu P.C.: Attenuation and velocity structure for site response analyses via downhole seismogram inversion. Pure Applied Geophysics 163 (1): 81-118 (2006).
112. Assimaki D., Li W., Steidl J.H., Tsuda K.: Site amplification and attenuation via downhole array seismogram inversion: A comparative study of the 2003 Miyagi-Oki aftershock sequence. Bulletin of the Seismological Society of America 98 (1): 301-330 (2008).
113. Cabas A., Rodriguez-Marek A., Bonilla L.F.: Estimation of site-specific Kappa (κ 0)-consistent damping values at KiK-Net sites to assess the discrepancy between laboratory-

based damping models and observed attenuation (of seismic waves) in the field. Bulletin of the Seismological Society of America 107 (5): 2258-2271 (2017).
114. Beresnev I.A., Wen K.-L.: Nonlinear soil response - A reality? Bulletin of the Seismological Society of America 86 (6): 1964-1978 (1996).
115. Shearer P.M., Orcutt J.A.: Surface and near-surface effects on seismic waves—theory and borehole seismometer results. Bulletin of the Seismological Society of America 77 (4): 1168-1196 (1987).
116. Borcherdt R.D.: Effects of local geology on ground motion near San Francisco Bay. Bulletin of the Seismological Society of America 60 (1): 29-61 (1970).
117. Hough S.E., Anderson J.G.: High-frequency spectra observed at Anza, California: implications for Q structure. Bulletin of the Seismological Society of America 78 (2): 692-707 (1988).
118. Tsai N.C., Housner G.W.: Calculation of surface motions of a layered half-space. Bulletin of the Seismological Society of America 60 (5): 1625-1651 (1970).
119. Dobry R., Whitman R.V., Roesset J.M.: Soil properties and the one-dimensional theory of earthquake amplification. MIT Department of Civil Engineering, Inter-American Program, (1971).
120. Joyner W.B., Warrick R.E., Oliver III A.A.: Analysis of seismograms from a downhole array in sediments near San Francisco Bay. Bulletin of the Seismological Society of America 66 (3): 937-958 (1976).
121. Ktenidou O.-J., Abrahamson N.A., Drouet S., Cotton F.: Understanding the physics of kappa (κ): Insights from a downhole array. Geophysical Journal International 203 (1): 678-691 (2015).
122. Kaklamanos J., Bradley B.A., Brandenberg S.J., Manzari M.T.: Insights from KiK-net data: What input parameters should be addressed to improve site response predictions? In: Geotechnical Earthquake Engineering Soil Dynamics V, Austin, 2018. pp 454-464
123. Stein S., Wysession M.: An introduction to seismology, earthquakes and Earth structure. (2003).
124. Tao Y., Rathje E.M.: Taxonomy for evaluating the site-specific applicability of one-dimensional ground response analysis. Soil Dynamics and Earthquake Engineering 128: 105865 (2020).
125. Huang D., Wang G., Du C., Jin F.: Seismic Amplification of Soil Ground with Spatially Varying Shear Wave Velocity Using 2D Spectral Element Method. Journal of Earthquake Engineering: 1-16 (2019).
126. Nour A., Slimani A., Laouami N., Afra H.: Finite element model for the probabilistic seismic response of heterogeneous soil profile. Soil Dynamics and Earthquake Engineering 23 (5): 331-348 (2003).
127. Toro G.R.: Probabilistic models of site velocity profiles for generic and site-specific ground-motion amplification studies. Brookhaven National Laboratory, Upton, New York (1995).
128. Passeri F., Aimar M., Foti S.: Modelli geostatistici per la valutazione delle incertezze e delle variabilità nei profili di Vs. In: Incontro Annuale dei Ricercatori di Geotecnica, Genova, Italy, 2018. Associazione Geotecnica Italiana,
129. Teague D.P., Cox B.R.: Site response implications associated with using non-unique Vs profiles from surface wave inversion in comparison with other commonly used methods of

accounting for Vs uncertainty. Soil Dynamics and Earthquake Engineering 91: 87-103 (2016).
130. Baise L.G., Dreger D.S., Glaser S.D.: The effect of shallow San Francisco Bay sediments on waveforms recorded during the Mw 4.6 Bolinas, California, earthquake. Bulletin of the Seismological Society of America 93 (1): 465-479 (2003).
131. Aimar M., Ciancimino A., Foti S.: An assessment of the NTC18 simplified procedure for stratigraphic seismic site amplification prediction. Italian Geotechnical Journal - Rivista Italiana di Geotecnica: (2020).
132. Hashash Y.M.A., Park D.: Non-linear one-dimensional seismic ground motion propagation in the Mississippi embayment. Journal of Engineering Geology 62 (1-3): 185-206 (2001).
133. Hashash Y.M.A., Musgrove M.I., Harmon J.A., Okan I., Groholski D.R., Phillips C.A., Park D.: DEEPSOIL 7.0, user manual. University of Illinois at Urbana-Champaign, (2017).
134. Darendeli M.B.: Development of a new family of normalized modulus reduction and material damping curves. Doctoral Dissertation, University of Texas at Austin, Austin, (2001).
135. Rollins K.M., Evans M.D., Diehl N.B., Daily III W.D.: Shear modulus and damping relationships for gravels. Journal of Geotechnical and Geoenvironmental Engineering 124 (5): 396-405 (1998).
136. Sun J., Idriss I.M.: User's manual for SHAKE91: a computer program for conducting equivalent linear seismic response analyses of horizontally layered soil deposits. Center for Geotechnical Modeling, Department of Civil Engineering, University of California, Davis, California (1992).
137. Passeri F., Foti S., Rodriguez-Marek A.: Geostatistical models for the assessment of the influence of shear wave velocity uncertainty and variability on ground response analyses. Paper presented at the 7th International Conference of Earthquake Geotechnical Engineering, Roma, Italy (2019).
138. Ministero delle Infrastrutture e dei Trasporti: DM 17/01/2018 - Aggiornamento delle "Norme Tecniche per le Costruzioni". (2018).
139. Foti S., Aimar M., Ciancimino A., Passeri F.: Recent developments in seismic site response evaluation and microzonation. In: Geotechnical Engineering, foundation of the future, Proceedings of the XVII ECSMGE, 2019. pp 223-248
140. Meletti C., Martinelli F. (2008) I dati online della pericolosità sismica in Italia. esse1.mi.ingv.it.